Report 1997:3

Climatic effects of NO_x emissions through changes in tropospheric O_3 and CH_4 A global 3-D model study

by

Jan S. Fuglestvedt[1], Terje K. Berntsen[1,2], Ivar S. A. Isaksen[1,2], Huiting Mao[3], Xin-Zhong Liang[3] and Wei-Chyung Wang[3]

[1]CICERO, University of Oslo, Norway
[2]Institute of Geophysics, University of Oslo, Norway
[3]Atmospheric Sciences Research Centre, State University of New York, Albany, USA

February 1997

ISSN: 0804-4562

Table of contents

SUMMARY

As a result of chemical processes in the atmosphere, emissions of NOx can both damp and enhance the greenhouse effect. The two most important effects of NOx in this context are increased concentrations of *tropospheric ozone* and reduced levels of *methane*. The ozone response has a warming effect (*positive* indirect effect) and the methane response gives cooling (*negative* indirect effect).

Previous studies using simplified models have shown that when NOx is emitted from ground sources, these effects may be of the same magnitude on a global scale. It is, however, important to be aware that since they have very different characteristics, these effects do not offset each other. In the free troposphere, the lifetime of ozone is 100-200 days and the changes in ozone and the resulting radiative forcing is limited to a regional scale. Changes in ozone and its radiative forcing occur relatively shortly after the emissions of NOx takes place. Methane, on the other hand, has a lifetime of 10-12 years and changes in methane degradation will therefore affect the concentration of methane on a global scale. The relatively long lifetime also leads to a corresponding time lag in the response of methane compared to changes in NOx emissions.

Studies of the effects of NOx have usually focused on the effects of increased emissions. In this project we have studied the chemical and radiative effects of *reduced NOx emissions*, and how these effects vary among different regions of the world. The following areas have been chosen: Scandinavia, Central Europe, Southern Europe, USA, Southeast Asia, and Australia.

In separate model tests the emissions of NOx have been reduced by 20% in each region, and the resulting changes in ozone and methane have been calculated. Changes in the concentrations of these gases have formed the basis for calculation of radiative forcing. In the case of Scandinavia it has been undertaken model tests where emissions of VOC and CO are also reduced. Calculations of the radiative forcing from both ozone and methane have been performed for Scandinavia (two tests), USA and Southeast Asia.

The results confirm earlier findings that the indirect effects of NOx through methane and ozone are of the same magnitude, but with opposite signs. We also find that the effects vary significantly in magnitude among the various regions. In addition, we find that in a global and regional perspective, 20% reductions in NOx emissions in Scandinavia have a negligible effect on climate.

The magnitude of NOx emissions in the studied regions varies substantially (a factor of 35 between USA and Scandinavia). This is due to differences in area size, population density, as well as economic and technological conditions. USA and Southeast Asia will experience the largest effect of a 20% reduction in NOx emissions on the concentrations of ozone and methane. This is due to the large emissions in USA and the chemical and meteorological conditions in Southeast Asia. Scandinavia separates from the rest by having the smallest effect.

The very large differences in changes in NOx emissions in absolute numbers necessitate a normalisation of the effects of changes in emissions; i.e. that changes in ozone and methane are calculated per Tg (10^{12} g) change in NOx emissions. The same has been done for radiative forcing (given as $W/m^2/TgN/yr$). A ranking of the regions according to changes in the most climate sensitive altitudes of *ozone concentrations per reduction in NOx emissions*, shows that Southeast Asia is the most sensitive area, followed by Australia. USA and Europe follow thereafter, with Scandinavia ranking slightly below. Concerning radiative forcing resulting from changes in *ozone* (radiative forcing per reduction in TgN), Southeast Asia is about 8 times more sensitive than Scandinavia, while USA is about 20% more sensitive.

We find that the sensitivity of radiative forcing due to increased methane concentrations is about 6 times higher for NOx reductions in Southeast Asia than for NOx reductions in Scandinavia. The sensitivity of NOx reductions in the USA is about 30% higher than in Scandinavia.

While the climate effect of a 20% reduction in NOx in Scandinavia is negligible, the radiative forcing of reductions in ozone resulting from a 20% reduction in NOx emissions in the USA is significant. However, if indirect radiative forcing of NOx reductions is given per unit reductions in NOx emissions, the estimates indicate that the sensitivities of radiative forcing from ozone and methane in Scandinavia and USA are comparable.

The estimates also show that changes in the emissions of other gases are very important. Model experiments that at the same time reduced the emissions of VOC and CO in Scandinavia by 30% (test 2) resulted in a radiative forcing of around 60% lower (less negative) than if only NOx emissions were reduced. The reason for this is that oxidation products from these gases take part in chemical reactions that remove ozone when NOx levels are sufficiently low. This fact underlines the need for considering various measures for emission reductions jointly and to analyse how measures affect several gases simultaneously.

A model experiment was also undertaken where emissions of VOC, CO and NOx were reduced by 30% in Scandinavia (test 3). The results showed only minor deviations from test 2 (20% reduction in NOx and 30% reduction in VOC and CO), but on a global scale the effect on ozone was somewhat lower in test 3. This is a result of complex relationships in the atmospheric chemistry as well as varying impacts of transport on the distribution of gases that leads to ozone formation. Reduced levels of NOx and O_3 and hence lower concentrations of OH in one region result in lower oxidation of CO and hydrocarbons. This in turn increases the supply of these ozone precursors in areas further south, and enhances the ozone levels there.

Because of the complex role of NOx in the chemistry of the atmosphere as well as large spatial and temporal variations in the NOx concentration, there are significant uncertainties associated with calculations of changes in ozone and methane. This implies that, at present, it is not possible to give any firm conclusions regarding the net effect of NOx on the radiative forcing, since the warming and the cooling effects are of the same magnitude. Estimations of net effects of NOx may be of limited value as the radiative forcing of ozone and methane have different characteristics and may lead to different effects on the atmospheric circulation patterns. Despite the uncertainties concerning quantification of indirect climatic effects of NOx emissions, several studies support our conclusion that NOx both has warming and cooling effects and that these probably are of the same magnitude. In order to study the chemical responses on changes in NOx emissions, we have used a global 3-dimensional model (longitude x latitude x elevation) with an extensive chemistry scheme as opposed to previous studies that used 2-D models. Radiative forcing resulting from changes in ozone is calculated by professor Wang and his group at the State University of New York at Albany, USA.

1. Introduction

Several studies have shown the importance of tropospheric ozone as a climate gas (e.g. Wang et al., 1980, and Lacis et al., 1990; Hauglustaine et al., 1994a,b). There are however some important differences between ozone and greenhouse gases such as CO_2 and N_2O since O_3 itself is not emitted in significant amounts, but is produced through chemical reactions in the atmosphere. Furthermore, due to a lifetime in the order of a few weeks to a few months depending on season and region, there are, in contrast to the long-lived gases, large spatial variations in the concentrations of ozone. Furthermore, the vertical distribution of changes in ozone is important since the climate sensitivity to ozone changes reaches a maximum in the upper troposphere and lower stratosphere (Wang et al., 1980; Lacis et al., 1990). Due to the relatively short lifetime and inhomogeneous distribution of changes in ozone, the pattern of effects on the radiative balance (i.e. radiative forcing, see definition below) will also show significant regional and temporal variations. This may in turn cause changes in the atmospheric circulation pattern.

Increases in free tropospheric ozone over the last 30 years are reported for several monitoring stations in the Northern Hemisphere. There are also indications of increases in ozone since the early 1900s. Observations and model studies together indicate that the amount of tropospheric ozone in the Northern Hemisphere may have doubled since pre-industrial times (IPCC, 1994, and references therein).

Several model studies indicate that longwave and shortwave changes in the radiative balance of the Earth/atmosphere have significant effects on climate. A change in average net radiation at the tropopause, due to a change in the fluxes of either longwave or shortwave radiation, has been defined as a *radiative forcing of climate* (IPCC, 1990, 1994). A radiative forcing disturbs the balance between incoming and outgoing radiation at the tropopause, but over time a new balance is established as climate responds to the radiative forcing. A *positive radiative forcing* means that more energy is trapped in the troposphere, and this will have a *warming* effect on the coupled troposphere-surface climate system. A *negative* radiative forcing will have a *cooling* effect.

For a doubling of the atmospheric concentration of CO_2 from the pre-industrial level, a global mean radiative forcing of about 4 W/m^2 has been calculated (IPCC, 1994). When feedback effects in the climate system are taken into account, model studies indicate increases in global average surface air temperature at equilibrium between 1.5 and 4.5 °C with a best estimate of 2.5 °C (IPCC, 1995).

Radiative forcing gives a first order estimate of the climate change potential of the mechanism under consideration. A radiative forcing of climate initiates a climate response, but there are significant uncertainties related to the magnitude of such responses since they are determined by several complex feedback processes. Radiative forcing can be calculated with more confidence and may thus serve as a useful indicator of climate change potential. But radiative forcing given as the global mean forcing or with a geographical resolution, does not indicate properly the three-dimensional pattern of the climate response. General circulation models (GCMs) are necessary to study the response of the climate system.

Gases that are emitted to the atmosphere (source gases) may influence the radiative balance *directly* due to their radiative properties (e.g. CO_2 and CF_4). Source gases such as CH_4 and NOx ($NO+NO_2=NOx$) may also give radiative forcing *indirectly* by changing the concentrations of other gases through chemical processes in the atmosphere. Important

climate gases such as tropospheric ozone and methane, may then be affected. The pathways giving radiative forcing of climate is illustrated in figure 1. The black arrows show the processes focused in this report.

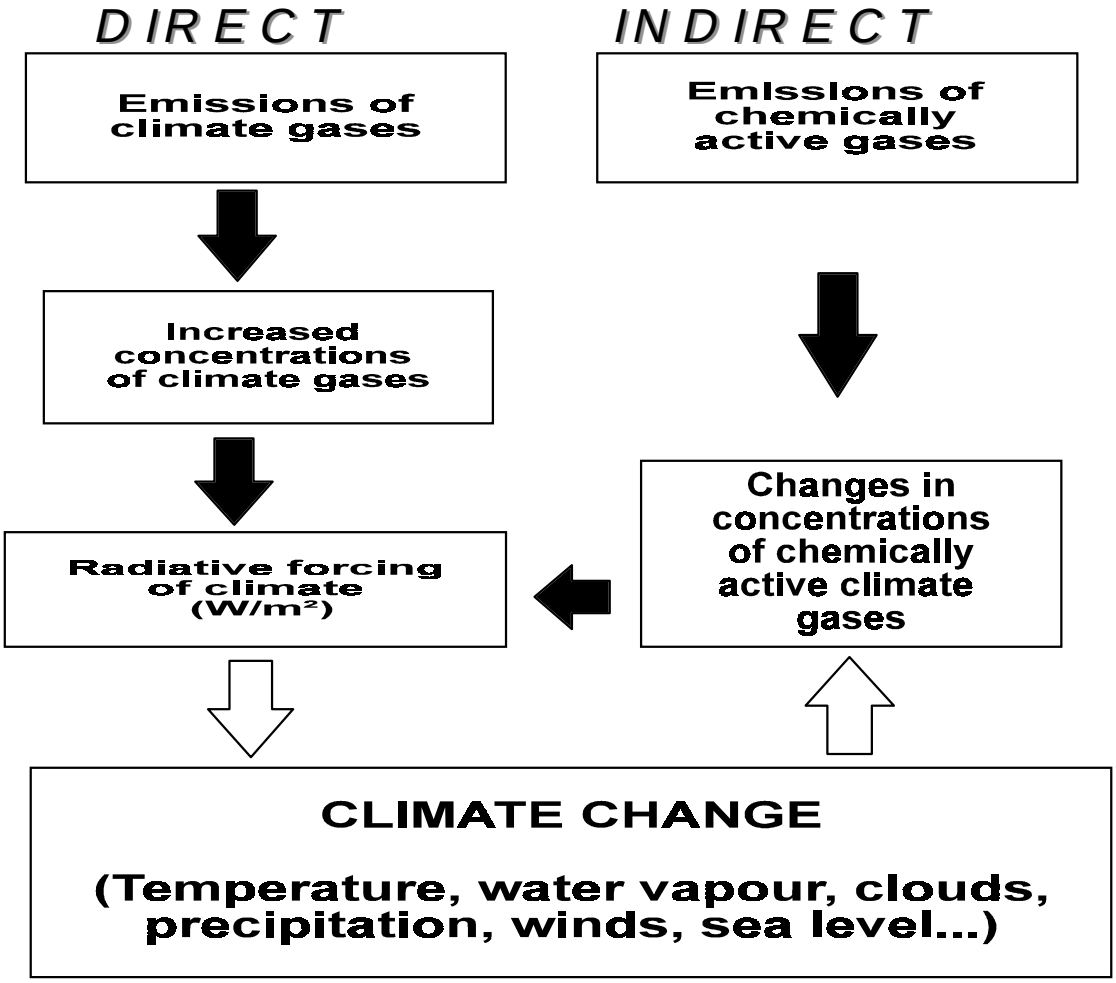

Figure 1. *The principles for direct effects, indirect effects and climate feedbacks through atmospheric chemistry. The filled arrows indicate the mechanisms considered in this paper. (From Fuglestvedt, 1995).*

There are several agents causing radiative forcing of climate. Figure 2 from IPCC 1995 shows the anthropogenically induced radiative forcing since pre-industrial times due to various emissions together with an estimate of the forcing due to solar variations. The largest single contribution is from CO_2 which gives a radiative forcing of 1.56 W/m^2. The total forcing from the well-mixed gases (CO_2, CH_4, N_2O, CFC-11, CFC-12, CFC-113, CCl_4, HCFC-22) is 2.45 W/m^2. Estimates of radiative forcing from changes in *tropospheric* ozone since pre-industrial times give positive radiative forcing of 0.2 to 0.6 W/m^2 (IPCC 1994 and references therein). For example, with a two-dimensional (2-D) model Hauglustaine et al. (1994a) have calculated changes in tropospheric ozone since pre-industrial times due to increased emissions which result in a global annual average forcing equal to 0.55 W/m^2, with the largest contribution at Northern mid-latitudes. With a three-dimensional model, Lelieveld and Dorland (1995) estimated a radiative forcing of 0.5 W/m^2 since pre-industrial times. Based on observations, Marenco et al. (1994) estimated a radiative forcing of 0.6 W/m^2 since pre-industrial times. Wang et al. (1993) used ozone observations at Northern middle and high latitudes to study the climate implications of ozone changes. Their results indicate that increases in tropospheric ozone may give a local positive radiative forcing comparable to the

effect of all other anthropogenically increased greenhouse gases. Berntsen et al. (1996b) estimated a global mean forcing of approximately 0.25 W/m^2 from ozone changes since pre-industrial times.

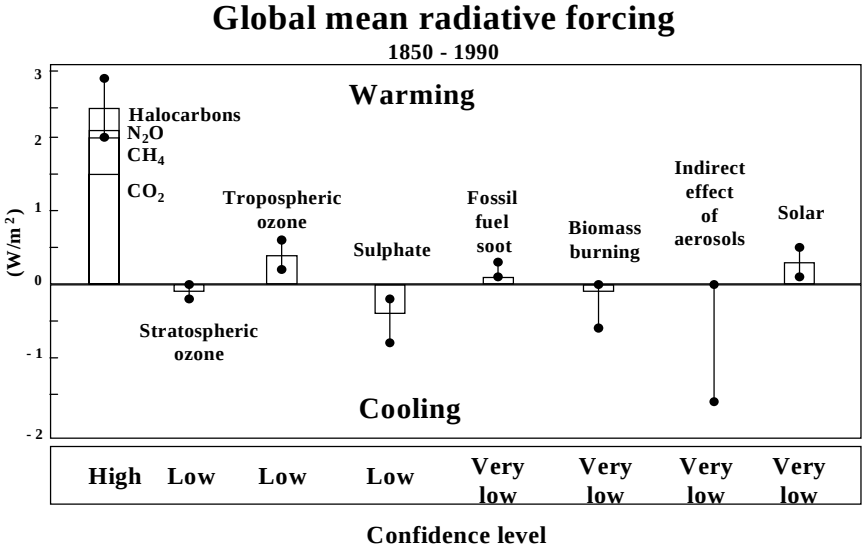

Figure 2. *Radiative forcing (in W/m^2) due to changes in the concentrations of climate gases and aerosols since pre-industrial times. The indirect effects of aerosols through changes in clouds are also indicated. The forcing from solar variations is given to the right. (From IPCC, 1995).*

Berntsen et al. (1996a) modelled the responses in ozone from increased emissions of NOx, NMHC and CO in Asia. Using the 1980 emissions as reference, the anthropogenic emissions were doubled, which is expected to occur by the year 2000. From the changes in ozone they calculated a radiative forcing of about 0.5 W/m^2 over large areas in Asia and a Northern Hemispheric average of 0.13 W/m^2. The regional forcing was almost as large as the negative forcing from sulphate in this region. The sulphate effect is for the period since pre-industrial time, while the estimated ozone effect is for a period of only two decades.

With respect to radiative forcing and climate change, NOx have a dual role (e.g. Isaksen and Hov, 1987; Fuglestvedt et al. 1993, 1996). Firstly, emissions of NOx generally increase the levels of tropospheric O_3. Secondly, NOx generally also increase the concentrations of OH radicals in the troposphere. Higher levels of tropospheric OH reduce the lifetimes of gases removed by reaction with OH. Several climate gases belong to this group, e.g. CH_4, HCFCs and HCFs. Emissions of NOx therefore lead to a *positive indirect effect* (i.e. warming) through ozone enhancements, and a *negative indirect effect* (i.e. cooling) through reduced lifetimes of methane and other climate gases removed by OH. The effects of NOx are not explicitly shown in figure 2. Increased emissions of NOx is one of the reasons for the higher ozone levels and the following forcing (a positive effect). In addition, the forcing from methane would have been larger without increased NOx emissions (a negative effect). With a 3-D model of the global troposphere, Lelieveld and Dorland (1995) calculated that the levels of CH_4 would have been approximately 30±5% higher than the present level without the increases in NOx emissions since pre-industrial times.

In IPCC (1990) the climate impact of NOx emissions on O_3 was given in terms of Global Warming Potentials (GWPs). The effect on the levels of methane was, however, not included. Later it was recognized that the magnitude of these indirect effects given in radiative forcing could be of similar magnitude, but of opposite sign (Isaksen et al. 1992; IPCC, 1992). The GWPs for NOx were left out in the IPCC assessments from 1992 and 1994 due to the large

uncertainties and insufficient scientific basis for drawing conclusions about the climate impacts of this gas. IPCC (1994) points to the large uncertainties regarding the effects of NOx on O_3 and the need for three-dimensional model studies of these relations.

As shown i.a. by Liu et al. (1987) and Lin et al. (1988) there is a strongly non-linear relation between the levels of NOx and ozone production. This is illustrated in figure 3 from a study by Liu et al. (1987) who find that for summer conditions at 40°N a molecule of NOx released in regions with 10 pptv of NOx (e.g. remote oceanic areas) will produce about 10 times as much ozone as a NOx molecule released in regions with more than 10 ppbv of NOx (e.g. urban areas). This means that NOx emitted or being transported to the remote troposphere is more efficient in producing ozone than if it were introduced to the troposphere in a industrialized region and oxidized there.

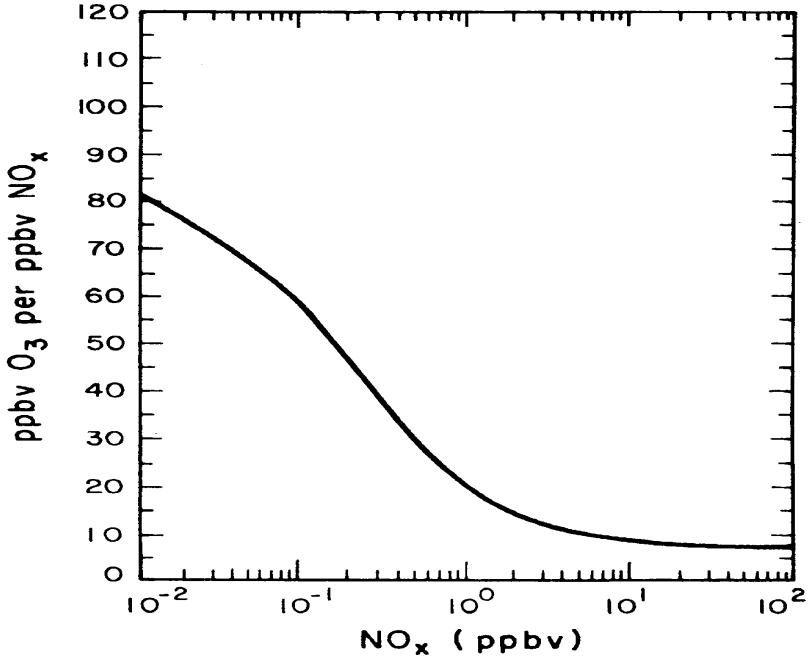

Figure 3. *O_3 increases per NOx molecule as a function of NOx levels. (From Liu et al. 1987).*

As shown by Crutzen (1987) the changes in O_3 and HOx that follows when CO and hydrocarbons are oxidized are dependent on the NO levels. In addition, the level of NOx also controls the distribution among the HOx ($HOx=OH+HO_2$) species (Berntsen et al., 1992) which is important since reaction with OH is the main sink for several climate gases.

In a 2-D model study by Fuglestvedt et al. (1996) the indirect effects from emissions of NOx from aircraft and surface sources, as well as for emissions of CH_4 and CO, were quantified in terms of changes in the concentrations of O_3 and CH_4 and further in terms of radiative forcing. For NOx emitted from *aircraft*, the positive radiative forcing from ozone changes was estimated to be significantly larger than the negative forcing from changes in CH_4. It was therefore concluded that the *net* effect of NOx emitted from aircraft is positive. Figure 4a shows the calculated radiative forcing from changes in tropospheric O_3 and CH_4 in response to a 70% increase in NOx emissions from aircraft. Contrary to the emissions from aircraft, *surface* emissions of NOx affect OH in a region of the troposphere that is very important for the oxidation of CH_4. As shown in figure 4b, the relative contribution from the negative effect through reductions in CH_4 is therefore larger than in the case of NOx emitted from aircraft. The estimated *net* forcing for a 10% increase in NOx emissions (with a fixed latitudinal emission profile), is slightly negative since the positive ozone forcing is somewhat smaller than the negative forcing from CH_4 reductions. It is important to note that this estimate of the effects of surface emissions of NOx depends on the geographical pattern of changes in emissions and the background levels of NOx, and that it may also be model dependent. These results should therefore be considered highly uncertain and preliminary. Nevertheless, the results point to the dual role of NOx emissions on climate gases in the troposphere.

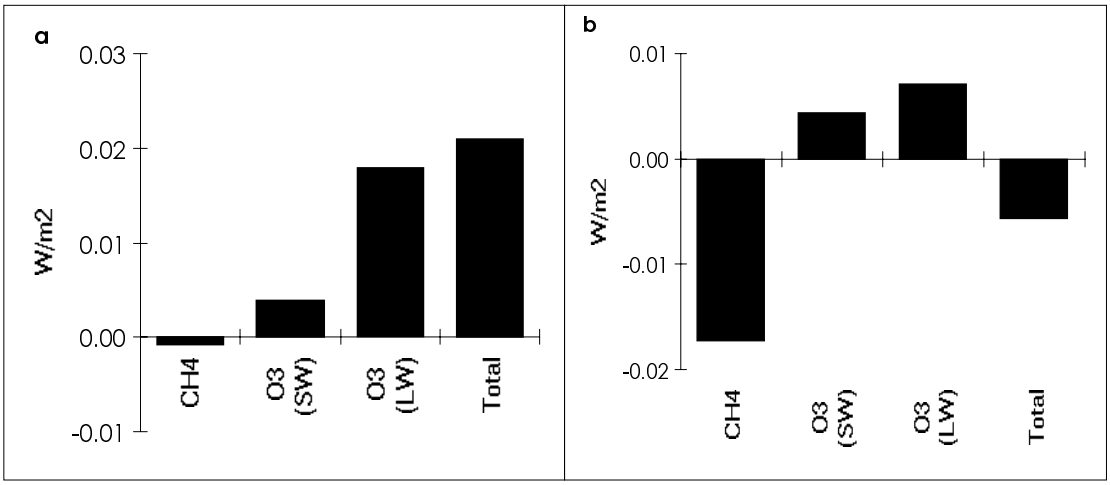

Figure 4. *Calculated radiative forcing from changes in tropospheric ozone (short wave (SW) and long wave (LW) forcing) and methane for a) 70% increase in NOx emissions from aircraft and b) 10% increase in NOx emissions from surface sources. (From a 2-D model study by Fuglestvedt et al., 1996).*

In Fuglestvedt et al. (1996) these calculations of radiative forcing formed the basis for estimation of GWPs for NOx from aircraft. For NOx from *surface* sources, however, it was concluded that the uncertainties were too large due to the use of a two-dimensional (2-D) chemistry-transport model of the global troposphere and the large dependence on the assumptions about where the increases in the emissions of NOx occur.

To illustrate *qualitatively* the dual role of NOx with respect to changes in climate gases and radiative forcing, *preliminary* Global Warming Potentials (GWPs) showing the effect of NOx from surface emissions on CH_4 and O_3 separately and the net effect, are given in figure 5.

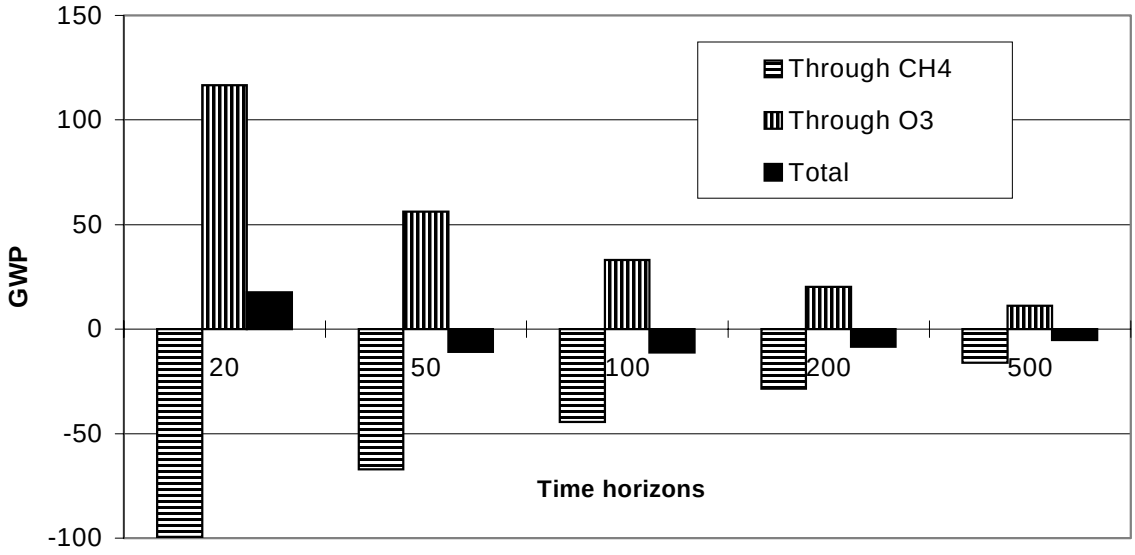

Figure 5. *Estimated GWP values for sustained emissions (SGWPs) of NOx from surface sources given for effect through CH_4 and O_3 separately and the total effect. The GWPs are given for various time horizons (years).(Based on Fuglestvedt et al., 1996).*

These highly preliminary 2-D model based GWP estimates illustrate the positive indirect effect of NOx through increased levels of tropospheric O_3, and the negative indirect effect through reduced levels of CH_4. It also shows that these two opposing effects occur on *different time scales*. The responses in O_3 occur rapidly, while the effect on methane is delayed due to the long chemical lifetime of this gas. The ozone effect dominates on shorter time scales giving a positive GWP for a time horizon of 20 years, while for longer horizons the negative effect through CH_4 dominates. The net effect is a difference between two numbers of similar magnitudes. Taking the large uncertainties into account we conclude that, based on the 2-D model study by Fuglestvedt et al. (1996), it is not possible to say whether emissions of NOx from surface sources in a global perspective have a positive or a negative net effect on climate through changes in O_3 and CH_4.

Lelieveld and Dorland (1995) studied the changes in ozone since pre-industrial times using a 3-D model and found that the emissions of NOx had given a positive radiative forcing through ozone changes that was of similar magnitude to the negative forcing through reduced lifetime of CH_4. Considering the large uncertainties, they also conclude that it is not possible to estimate a global average climate forcing from NOx emissions.

Other studies have also shown the dual role of NOx emissions. Using a global 2-D model Hauglustaine et al. (1994b) calculated a radiative forcing of $1.5 \cdot 10^{-2}$ W/m^2 from O_3 changes in response to the present emissions of NOx from aircraft. The changes in CH_4, on the other hand, gave a radiative forcing equal to $-4.2 \cdot 10^{-3}$ W/m^2, corresponding to -28% of the O_3 forcing. Johnson (1994) estimated a negative radiative forcing from CH_4 changes in response to NOx from aircraft of about 10% of the O_3 forcing. Calculations by Johnson (1994) and Derwent (1994) also shows a significant negative forcing from surface emissions of NOx through reductions in CH_4, counteracting the positive forcing from O_3 changes. Johnson and Derwent (1996) calculated sustained GWPs for NOx and found a *net* positive global warming potentials for NOx emitted in the Northern Hemisphere. For a time horizon of 100 years the SGWP[1] was estimated to 5. For the Southern Hemisphere, on the other hand, the

[1] Global Warming Potential for a sustained increase in emission and not for a pulse emission.

corresponding global warming potential was -10. The authors emphasise the uncertainties in their calculations, but the results nevertheless points to the potential significance of NOx in the context of climate change.

In all these studies, except the study by Lelieveld and Dorland (1995), 2-D models were applied and the spatial variations in gases are calculated as function of altitude and latitude. This is a critical simplification due to the large zonal (east-west) variations in several important key species in the chemistry of the troposphere. NO is one of these key species, and plays a very important role in the chemistry controlling O_3 and OH. There are large zonal variations in the emission intensity of NOx and thereby also in the atmospheric concentrations since the lifetime of NOx is only a few days or less, while the zonal transport time is approximately 2 weeks. By using 2-D models and assuming zonal homogeneity, the ability to model some important non-linear effects in tropospheric chemistry is reduced.

Observations and model studies show that there are large variations in the NOx levels not only at the surface, but also in the free troposphere due to efficient convective transport and that there is a close relation between the NOx levels and the net production of O_3. Due to the nature of the sources of NOx, the concentrations of NOx are largest over the continents.

Several studies have shown that indirect chemical effects of emissions have significant effects of global radiative forcing of climate (e.g. Hauglustaine et al., 1994a; Berntsen et al., 1996b; Fuglestvedt et al., 1996). Quantifications of such effects are necessary for formulating comprehensive approaches for controlling anthropogenic perturbations of climate. The motivation for this project is to improve our understanding of the climatically relevant responses to NOx emissions and to be able to estimate quantitatively the *net* effect on climate and understand how this net effect varies with the location of the changes in emissions. The main improvement relative to the 2-D model study by Fuglestvedt et al. (1996) referred to above, is that we use a three-dimensional (3-D) model with a convective transport scheme. This model enables us to take the large zonal variations in the NOx levels into account. Changes in the levels of tropospheric O_3 and CH_4 in response to emissions of NOx from surface sources will be focused. Since CH_4 (and several other climate gases) are controlled by OH, the responses in the OH fields are also studied. The model is developed by Berntsen and Isaksen (1996) and applied i.a. by Berntsen et al. (1996a), see chapter 3.

The overall objective is to obtain more reliable estimates of the impacts of emissions of NOx from surface sources on climate through the responses in tropospheric O_3 and CH_4. How the climate impacts, quantified in terms of radiative forcing, vary with geographical location of the emission changes will be focused. We will focus on monthly mean values of ozone since this gas is studied in the context of climate effects. The effects of changes in NOx, CO and VOC emissions on episodes with high concentrations of surface ozone will not be considered.

2. Methodological approach

First we will focus on the importance of location of surface emissions of NOx for the responses in O_3 and OH. Since reaction with OH is the main loss for CH_4 we will also study the changes in the OH fields due to NOx emissions and estimate the changes in the global average level of methane. To study the importance of geographical location for the chemical responses we define 6 regional groups as given below.

Group 1: Australia
Group 2: Southern Europe
Group 3: Central Europe
Group 4: Scandinavia
Group 5: Southeast Asia
Group 6: USA

Figure 6 shows the location of the groups defined above.

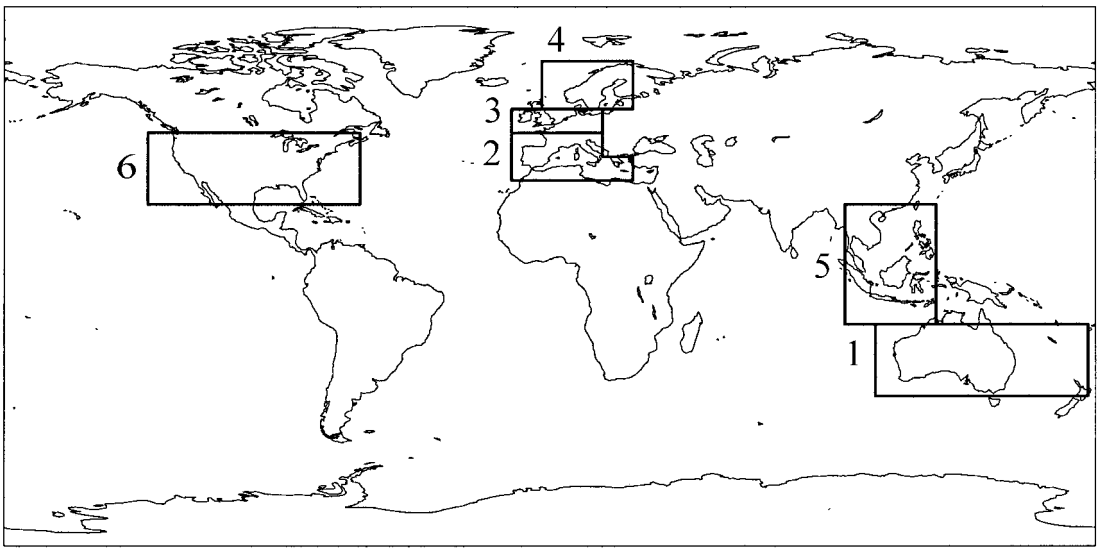

Figure 6. *The location of the groups where the emissions are changed.*

How ozone responds to *simultaneous* changes in the emissions of several gases is also studied and three types of tests are performed:

Test 1: The emissions of NOx are *reduced by 20%* in the region under consideration.

Test 2: The emissions of NOx *reduced by 20%* while the emissions of VOC and CO are *reduced by 30% each*, in the region under consideration.

Test 3: The emissions of NOx, VOC and CO are *reduced by 30% each* in the region under consideration.

We have also performed a model test where the NOx emissions in *all* the groups were reduced by 20% simultaneously. Table 1 gives the emissions and the changes in the surface emissions of NOx in the various groups.

Group:	**1 Aust-ralia**	**2 S-Europe**	**3 Central Europe**	**4 Scand-inavia**	**5 South-east Asia**	**6 USA**	**Total group 1-6**	**Global**
NOx emission ($TgNO_2$/yr)	2.77	6.46	7.29	0.70	3.88	24.73	45.84	115.7
NOx emission (TgN/yr)	0.84	1.97	2.22	0.21	1.18	7.53	13.96	35.2
Emission reduction (-20%) $TgNO_2$/yr	0.555	1.292	1.458	0.140	0.777	4.947	9.17	
Emission reduction (-20%) TgN/yr	0.169	0.393	0.444	0.043	0.236	1.506	2.79	
Emission reduction in % of global	0.48	1.12	1.26	0.12	0.67	4.28	7.92	

Table 1. *Changes in total surface emissions of NOx in the geographical groups under consideration.*

The modelled changes in the concentrations of ozone and methane will be given both in absolute terms and normalised to the changes in NOx emissions.

The modelled changes in O_3 and CH_4 fields have formed the basis for calculations of radiative forcing of climate. Radiative forcing is calculated for changes in emissions at various geographical locations. Sensitivity factors for the different regions (given as radiative forcing per change in NOx emissions) have been calculated in order to show the geographical variations in radiative forcing in response to changes in the emissions of NOx. In addition, the global annual average radiative forcing is also calculated.

By testing out the effect of NOx emissions in a global 3-D chemistry/transport model, we will obtain a more detailed and scientifically sound understanding of the climate impacts of NOx than what was possible in previous studies where mainly 2-D models were applied. While 2-D models neglect the east-west variations in NOx, 3-D models are able to resolve much of these NOx variations. Lelieveld and Dorland (1995) used a 3-D model to study the changes in ozone since pre-industrial times, while this work focuses on how the effects of NOx reductions on O_3 and CH_4 varies between different geographical regions.

3. The models

3.1 The chemistry/transport model

The 3-dimensional (3-D) global model is based on the 3-D Chemical Tracer Model (CTM) developed at NASA/GISS (Prather et al., 1987), with the incorporation of an extensive chemical scheme to calculate transport and chemical transformation of species affecting the photochemistry in the troposphere. A detailed description of the model is given in Berntsen (1994). The model horizontal resolution is 8º latitude x 10º longitude. There are 9 vertical layers (σ-coordinates) from the surface to 10 hPa. The σ-coordinates are defined by $\sigma = (P-P_{top})/P_s$ where P_{top}=10 hPa, and P_s is the air pressure at the surface. The upper two layers (above about 14 km altitude) considered to be in the stratosphere, are treated as boundary conditions, with pre-set, climatological concentrations of ozone, NOx and HNO_3 species. The internal transport in the model will then generate the appropriate cross tropopause fluxes.

A one year simulation of meteorological data from the NASA/GISS GCM (Hansen et al., 1983) is used as input to the model. The GCM calculations are done with a horizontal resolution of 4º latitude x 5º longitude, and data from four boxes are then mapped into one to give the 8ºx10º resolution of the CTM. The data includes (i) 8-hourly mean winds at the boundaries of each gridbox, (ii) 8-hourly surface pressures, 8-hour totals of convective events (separately shallow wet, deep wet and dry), total optical depth and precipitation in each grid column, (iii) 5-day mean temperatures and humidity in each gridbox, and (iv) 5-days means of the detailed pattern of convective frequencies (dry, shallow wet and deep wet) between individual pairs of vertical layers in each grid square column.

The model solves the 3-D continuity equation of tracer concentration with one hour timesteps. The advection is solved by an upstream method with conservation of first- and second-order moments of concentration (Prather, 1986). The distribution of tracers within each gridbox is described by a second-order polynominal in three directions. This yields a very accurate calculation of the advective tracer transport, with very low numerical diffusion. The vertical convection of tracers is calculated every hour by using the total convective mass fluxes for each 8ºx10º grid cell as recorded every 8 hours in the CTM's history of meteorological fields. The tracers are assumed to follow the redistribution (updrafts and subsidence) of air unless wet removal of soluble species is allowed (Russel and Lerner, 1981). Observations and analysis show (Lelieveld et al., 1989, Pickering et al., 1992) that deep convective cells are able to transport air from the boundary layer to the upper troposphere with a time scale of 10-15 minutes. This is short enough to allow for transport of short lived tracers emitted at the ground, to the upper troposphere.

3.1.1 Chemistry

The chemical scheme which is used in the model, and how the time dependent equations are solved are described in detail in Berntsen (1994). It is based on the scheme used extensively in 2-D models for ozone chemistry and perturbation studies (Isaksen, 1980; Isaksen and Hov, 1987; Berntsen et al., 1992; Fuglestvedt et al., 1994). The diurnal variations of approximately 50 chemical compounds are calculated, of which 25 are transported. The set of coupled differential equations in the chemical scheme is solved with a QSSA-method (Hesstvedt et al., 1978) with a time step of 30 minutes. However, an iterative procedure is applied to the shortlived HO_x-species ($HOx=OH+HO_2$) which increases the accuracy of the scheme

considerably (Hesstvedet et al, 1978; Hertel et al., 1993). The calculations include a full diurnal cycle in photodissociation rates.

The model use pre-calculated photodissociation rates (J-values) derived with the two-stream approximation method of Isaksen et al. (1977), with modifications described in Jonson and Isaksen (1991) to improve the description of diffuse radiation from Rayleigh scattering and scattering by clouds and aerosols. In the model a distribution of clouds is inferred from the data for total optical thickness from the GCM-model (with 8-hour time resolution). The J-values are then interpolated from a set of J-values with different assumptions of the cloud distribution (Berntsen, 1994).

The primary production of odd-hydrogen ($OH+HO_2$) in the troposphere is through the reactions:

$O_3 + h\nu \rightarrow O(^1D) + O_2$ R1

$O(^1D) + H_2O \rightarrow OH + OH$ R2

The distribution between the odd-hydrogen species, and thereby the actual concentration of OH, is largely determined by the NOx concentrations through:

$NO + HO_2 \rightarrow NO_2 + OH$ R3

$NO_2 + OH + M \rightarrow HNO_3 + M$ R4

In polluted regions with high photolytic activity, reaction R3 and subsequent photolysis of NO_2 leading to ozone formation, will increase the OH/HO_2 ratio significantly. This is the major reason for the OH maximum found over polluted regions during summer (figure 9), even if emissions of CO and NMHCs, which consumes OH, are high. When photodissociation rates are slower or if the levels of NO_2 are very high, reaction R4 becomes increasingly important as a loss reaction for odd-hydrogen, and similar OH-maxima are not found (Poppe et al., 1993).

In background regions in the marine boundary layer and in the lower free troposphere (2-6 km) NOx concentrations are normally very low, and reactions other than R3 involving HO_2 becomes important. Radical - radical reactions which constitutes a loss of odd-hydrogen becomes important, i.a. :

$HO_2 + HO_2 \rightarrow H_2O_2 + O_2$ R5

$RO_2 + HO_2 \rightarrow ROOH + O_2$ R6

A significant part of the peroxides thus formed are dissolved in cloud droplets and lost through wet deposition. In the “low NOx” environment (NO less than 5-10 pptv), there is a net loss of odd-hydrogen and ozone through oxidation of methane and other hydrocarbons, while odd-hydrogen is actually produced in more polluted regions (Crutzen, 1987). The reactions leading to ozone loss are:

$O_3 + HO_2 \rightarrow OH + 2O_2$ R7

$O_3 + OH \rightarrow HO_2 + O_2$ R8

To simulate the global distribution of OH and the net ozone production with a model, it is therefore important to be able to resolve both regionally polluted regions and the cleaner background regions properly. 3-D models take into account the large variations along the east-west dimension.

3.1.2 Removal processes

Pollutants emitted to the atmosphere are transported and processed chemically and by radiation, before being removed form the atmosphere. The two basic removal processes in the model are through dry deposition at the surface and through scavenging of soluble species by rain. In the model the rate of dry deposition is parameterized through application of dry deposition velocities, which incorporates surface resistance (i.e. how easy the components stick to the surface, or is taken up by vegetation), laminar layer resistance (i.e. transport through the approximately 1 mm thick laminar layer closest to the ground) and boundary layer resistance (i.e. transport through the boundary layer by turbulens). Scavenging by rain is dependent on the precipitation (i.e. rates at each vertical layer) and the solubility of the species. In the model the following species are removed by rain: HNO_3, H_2O_2 , ROOH, and all carbonyl species. See Berntsen (1994) or Berntsen and Isaksen (1997) for a description of the model.

3.1.3 Emissions

This model is not only intended to simulate the observed composition of photochemically active species in the atmosphere (and thereby improve our understanding of the atmosphere), but also to be a tool which can be used to evaluate the effects of changes is emissions of certain components. However, since the photochemistry of the troposphere is highly non-linear, the model can not do a proper job in the second task, if it is not doing well in the first task. In particular is the model distribution of NO_x important. To simulate the observed distribution of species a good database of the emissions is obviously needed. The globally and annually averaged emissions applied in the model is given in table 2. The NOx-emissions (with a regional distribution) are obtained from Dignon et al. (1992) for the anthropogenic and biomass burning part. NOx emissions from lighting is distributed according to the deep convective activity in the meteorological data with a total of 5.2 TgN/year. Emissions from aircraft (total 0.6 TgN/year) are obtained from British Aerospace (with a 3-D distribution).

Species	Surface emissions		Lightning	Total
	Anthropogenic	Natural		
NO (TgN/yr)	21.8	12.4	5.2	39.4
NO_2 (TgN/yr)	0.65	0.37		1.02
CO (Tg/yr)				1575
C_2H_6 (Tg/yr)	22.6	14.4		37.0
C_4H_{10} (Tg/yr)	15.5	14.4		29.9
C_6H_{14} (Tg/yr)	17.1	7.2		24.3
C_2H_4 (Tg/yr)	22.3	14.4		36.7
C_3H_6 (Tg/yr)	19.8	7.2		27.0
m-Xylene (Tg/yr)	15.5	7.2		22.7
HCHO (Tg/yr)				1.11
Isoprene (Tg/yr)		205		205

Table 2. *Total annual emission rates applied in the model.*

Emissions of CO are treated by assuming that the sources have the same distribution as the NOx sources, with a total source strength taken from Hough (1991). Nevertheless, comparison with observations have shown that the model results for CO and O_3 are generally very good (Berntsen and Isaksen, 1997). The sources of non methane hydrocarbons (NMHCs, or VOC) are not as well known as for the other components, in particular are the natural sources poorly known. The database used as input in the model is taken from on Watson et al. (1990) for anthropogenic emissions and Isaksen and Hov (1987) for the biogenic part. Natural emissions are restricted to the continents.

3.2 Radiative model

The radiative forcing from the modelled ozone changes is calculated using the radiation code from SUNYA/NCAR GENESIS model (Thompson et al., 1995). The radiative forcing due to ozone changes is calculated by comparing changes in the net radiation flux (the solar and longwave radiation fluxes) at the tropopause between two sets: the reference set with SUNYA ozone climatology and the second one with imposed percentage changes of ozone derived from Oslo data on SUNY ozone climatology. The other inputs which include temperature, moisture, cloudiness, incoming solar radiation and surface albedo are based on the climate model simulations of present climate documented in Wang et al. (1995), and all these parameters are functions of latitude, longitude and altitude as well as season.

4. Results from chemistry calculations

4.1 Reference distributions of chemical species

To study the effects of changes in emissions, a model run with the present emissions was performed in order to have reference distributions for comparison with the modelled distributions in the perturbed case. Figure 7 shows the modelled monthly mean distribution of NOx (pptv) in the reference run for the lowest layer (L = 1) and for approximately 12 km (L = 7) for June and December.

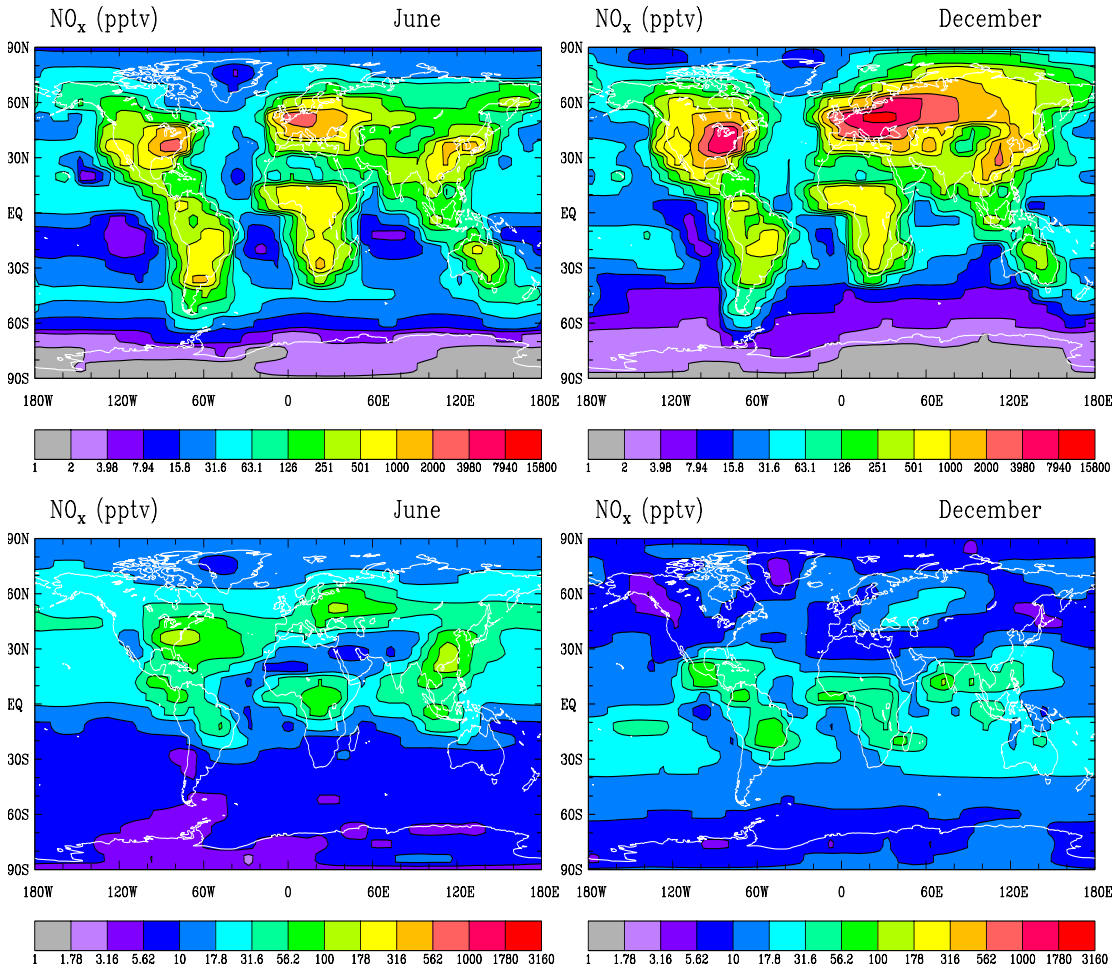

Figure 7. *Modelled distributions of NOx (pptv) in the reference case for the lowest layer in June (upper, left), and December (upper right) and for approximately 12 km in June (lower left) and December (lower right).*

Due to the short lifetime and the large geographical variations in the emission rates of NOx, there are large spatial and temporal variations in the concentrations of this gas. In remote regions the NOx levels are as low as a few pptv in the lowest model layer. These regions are generally over the oceans at low latitudes. Over the continents the NOx levels are much higher, especially over the polluted regions where they reach several ppbv. In the upper

troposphere (the two lower figures in the panel) the regional variations are somewhat less pronounced, but still the effects of surface emissions can be seen due to effective vertical transport from the surface. The large variations are important for the chemical responses to changes in emissions since NOx is a key species is several chemical processes. As shown in figure 3, there is a strong non-linear relation between ozone production and NOx levels. Thus, regional variations in the chemical responses to changes in NOx emissions may be expected.

Figure 8 shows the modelled distribution of O_3 (ppbv) in the reference run for the lowest layer (L = 1) and for approximately 12 km (L = 7) for June and December. The figures show that the ozone distribution broadly follows the NOx distribution in June, although the effect is somewhat smoothed out spatially due to the longer lifetime of ozone. During winter-time in the Northern Hemisphere, the high NOx concentrations over the polluted regions supress ozone concentrations over Europe and northern parts of USA. Emissions from southern USA, Mexico and Southeast Asia give ozone production even during winter giving an ozone maximum around 20-30°N. In the upper troposphere the O_3 levels are much higher due to the transport from the stratosphere. Efficient upward transport in the tropics (upward branch of the Hadley cell) brings up surface air with very low O_3 concentrations to the upper troposphere, and supress downward mixing of ozone rich air from the stratosphere.

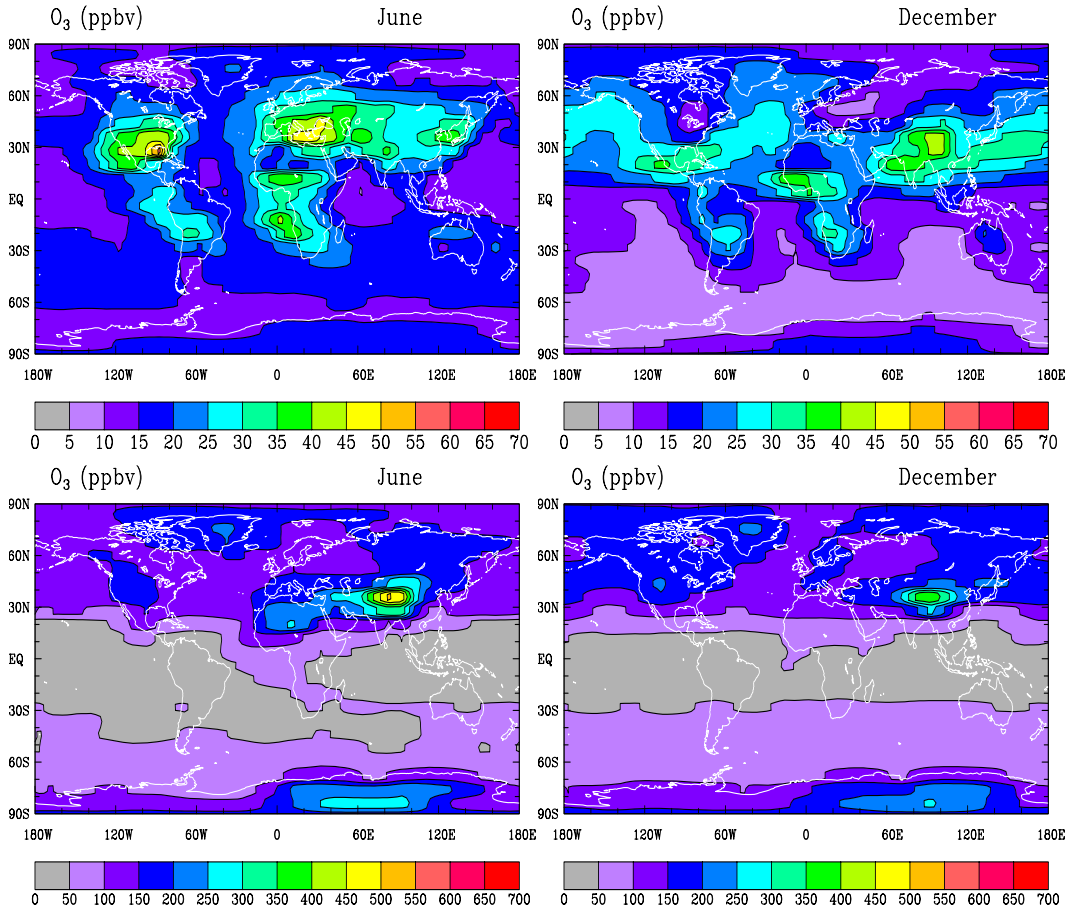

Figure 8. *Modelled distributions of O_3 (ppbv) in the reference case for the lowest layer in June (upper, left), and December (upper right) and for approximately 12 km in June (lower left) and December (lower right).*

Figure 9 shows the modelled distribution of OH (molecules/cm^3) in the reference run for the lowest layer (L = 1) for June. The OH levels are highest at latitudes with strong solar insolation and high humidity (see reactions R1 and R2). The OH levels are also higher over the continents due to higher O_3 and NOx levels here. The marked increase in OH at low latitudes are important for the spatial distribution of the methane oxidation. Except for dessert regions, high OH levels correlate with high temperatures which make low latitudes important for oxidation of CH_4 and other hydrocarbons. Due to the reduction in temperature and air density with height, most of the oxidation occurs in the lower troposphere. This means that OH changes at low altitudes and low latitudes are most important for changes in methane.

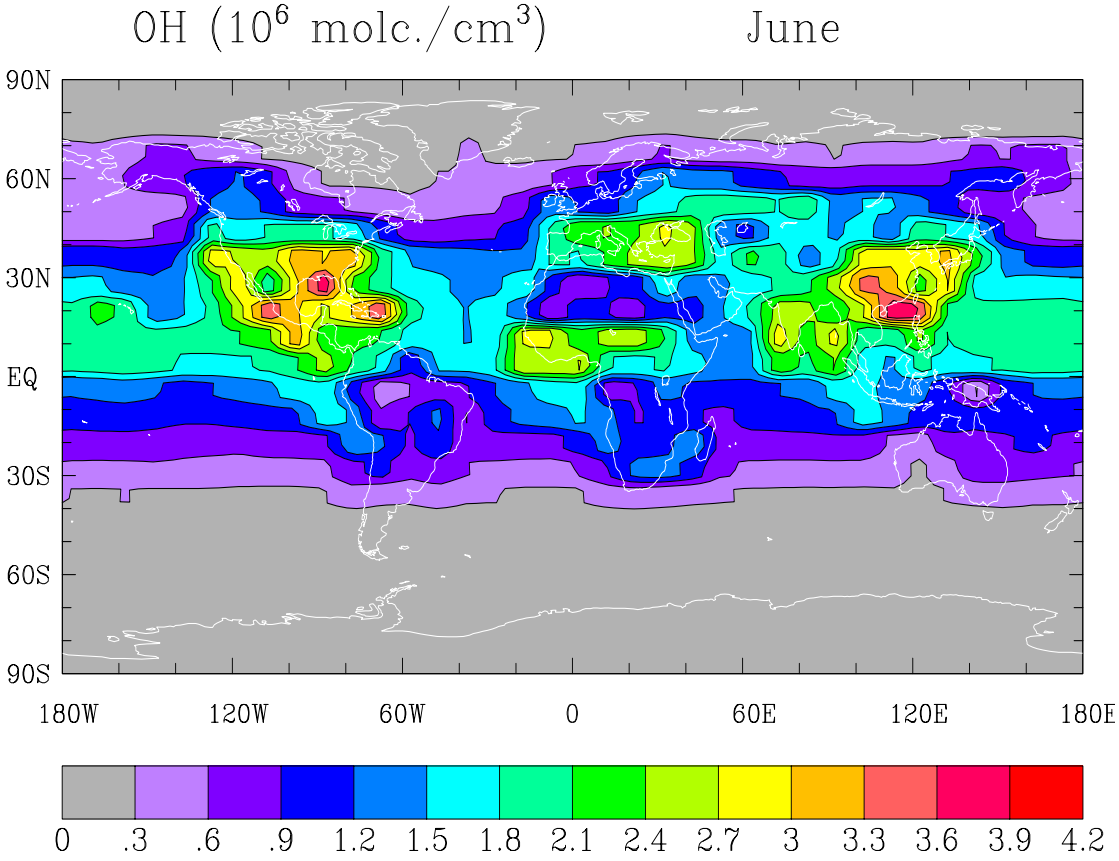

Figure 9. *Modelled distribution of OH in the reference case for the lowest layer in June.*

4.2 Changes in ozone

Changes in the surface emissions of ozone precursors will influence ozone in at least two different ways which are of interest from a pollution control point of view. Ozone in the atmospheric *boundary layer* (from the surface to about 2 km) have direct adverse effects on plant growth, materials and human health. In addition, ozone in the *free troposphere* will be affected, and such changes cause radiative forcing of climate. With regard to radiative forcing of climate, the vertical distribution of the ozone changes is very important. Since the greenhouse effect is strongest when terrestrial radiation from the surface is absorbed and re-emitted from a layer in the atmosphere where temperatures are lower, changes in ozone concentrations around the temperature minimum at the tropopause height will give the largest radiative forcing (Wang et al., 1980; Lacis et al., 1990). Calculated changes in ozone

concentrations in the surface layer of the model (L=1, ca. 0.25 km) and in the upper free troposphere (L=7, ca. 12 km) are presented in appendix 1.

For the responses in the *boundary layer* the regions can be separated in two groups. For group 5 (Southeast Asia) and group 1 (Australia), 20% reductions in the surface NOx emissions cause reduction in surface ozone levels in all seasons of the order of 5-10%. The effect is always less than 1% outside the region itself (see figure 1 and 5 in the Appendix). For northern mid-latitude regions, on the other hand (group 2, 3, 4 and 6), the effect on surface ozone is of opposite sign during winter due to the high background NOx levels and a significant seasonal cycle in solar insolation. During winter, the ozone concentrations tend to *increase* when NOx emissions decrease (up to 12% increase over USA in December). This is caused by the following mechanism:

$NO + O_3 \rightarrow NO_2 + O_2$ R9

$NO_2 + O_3 \rightarrow NO_3 + O_2$ R10

$NO_2 + NO_3 + M \rightarrow N_2O_5 + M$ R11

$N_2O_5 + H_2O$ (on wet aerosols) $\rightarrow 2HNO_3$ R12

The HNO_3 thus formed is water soluble and is readily scavenged by rain. This mechanism is efficient if solar radiation is low so that the photolysis reactions

$NO_2 + h\nu \rightarrow NO + O$ R13

$NO_3 + h\nu \rightarrow NO_2 + O$ R14

are slow, if background NOx levels are high so that N_2O_5 is formed by R11 (the rate of formation is approx. quadratic in NOx since the NO_3 concentration is controlled by NO_2), if temperatures are low so that thermal dissociation of N_2O_5 is slow and finally if the number of aerosols are high. All this factors are present at mid and high latitudes during winter. A reduction of NOx emissions will thus tend to increase ozone over this regions during winter. Over the most polluted regions in Europe (group 3) this effect is working even during June due to high levels of NOx and aerosols. The stronger solar radiation and the lower NOx levels in the southern parts of group 2 (Southern Europe) and group 6 (USA), give environments more similar to what is found for group 1 (Australia), and decreases in ozone are calculated during winter. During summer the reductions in NOx emissions generally cause a decrease in the surface ozone concentrations up to 10% close to the surface sources in group 2 and 6.

In the *upper free troposphere* the effect is always to decrease ozone concentrations (or very minor increases, mostly due to numerical noise). The impact becomes much more smoothed out than in the boundary layer, due to longer lifetimes of ozone and its precurcors, as well as more rapid zonal transport. For group 5 (Southeast Asia), which by the definition applied in this study is located in the tropics), the impact is not smoothed out to any significant degree. The percentage change in the mixing ratio of ozone is lower in the upper free troposphere than in the maximum region at the ground. Since the mixing ratios generally increase with hight, the absolute differences between the changes in the upper and lower troposphere will be smaller. From a climatic point of view, the larger area affected by the changes in ozone in the upper free troposphere are important for the global radiative forcing.

The two combined tests (test 2 and test 3) performed for Scandinavia (group 4) in which VOC and CO emissions are decreased as well, show very small differences for the boundary layer ozone concentrations compared to test 1. This underlines that VOC and CO concentrations in Scandinavia are less influenced by local sources than what is the case for NOx.

In the upper free troposphere there are very pronounced differences between test 2/test 3 and test 1. In test 2 and 3, ozone concentrations increase north of about 40°N during summer, while there is a decrease in the tropical regions, while in test 1 ozone decrease north of about 40°N and is virtually unchanged in the tropics. At the higher latitudes the decreased amount of peroxy radicals (RO_2 and HO_2) in test 2 and 3 produced through CO and VOC oxidation, gives less chemical loss of ozone through

$HO_2 + O_3 \rightarrow OH + O_2$ R7

while in the tropical region the reaction

$HO_2 + NO \rightarrow OH + NO_2$ R3

which gives ozone production through

$NO_2 + hv \rightarrow NO + O$ R13

$O + O_2 + M \rightarrow O_3 + M$ R15

is more important due to higher NOx levels and stronger solar insolation. Due to short lifetime, the NOx changes in Scandinavia will not affect the ozone levels south of approximately 40°N. Changes in CO and VOC, however, will affect a larger area due to longer lifetimes. Lower supply of these ozone precursors south of approximately 40°N will reduce the production and concentration of ozone here.

The climate impact of the calculated ozone changes will i.a. be presented as annual averaged radiative forcing (section 5.2). Factors that control this forcing are the magnitudes of the changes in ozone concentrations in the upper free troposphere as discussed above, but also the annual cycles of the changes. The degree of change in the upper free troposphere is dependent on the total change in surface sources, but also is also crucially dependent on the efficiency of the vertical mixing in the troposphere. The vertical mixing is caused mainly by rapid transport through deep convective clouds, which brings ozone precursors aloft and gives rise to increased in situ ozone production (Berntsen et al., 1996a). There are considerable differences in the seasonal cycle of deep convective activity between the regions in this study.

As shown in table 1 there are large differences in the magnitudes of the emission changes between the various groups. In order to compare the responses and the sensitivities of the responses between the groups, the ozone changes are divided by the change in NOx emission. A sensitivity factor α is then defined as:

$$\alpha_i^L = \frac{\Delta \overline{O}_3^L}{\Delta E_{i\ NOx}} \left(\frac{ppbv}{TgN\ /\ yr} \right)$$

where L is the layer in the model and i is the group where the emissions are reduced. The changes in ozone ($\Delta\overline{O}_3^L$) are given as change in global mean for each model layer. L=1 is about 250 m, L=4 is about 3.5 km, and L=6 and 7 is 8.5 km and 12 km, respectively. Figure 10 shows calculated values of α for the different tests for the selected altitude levels as function of month.

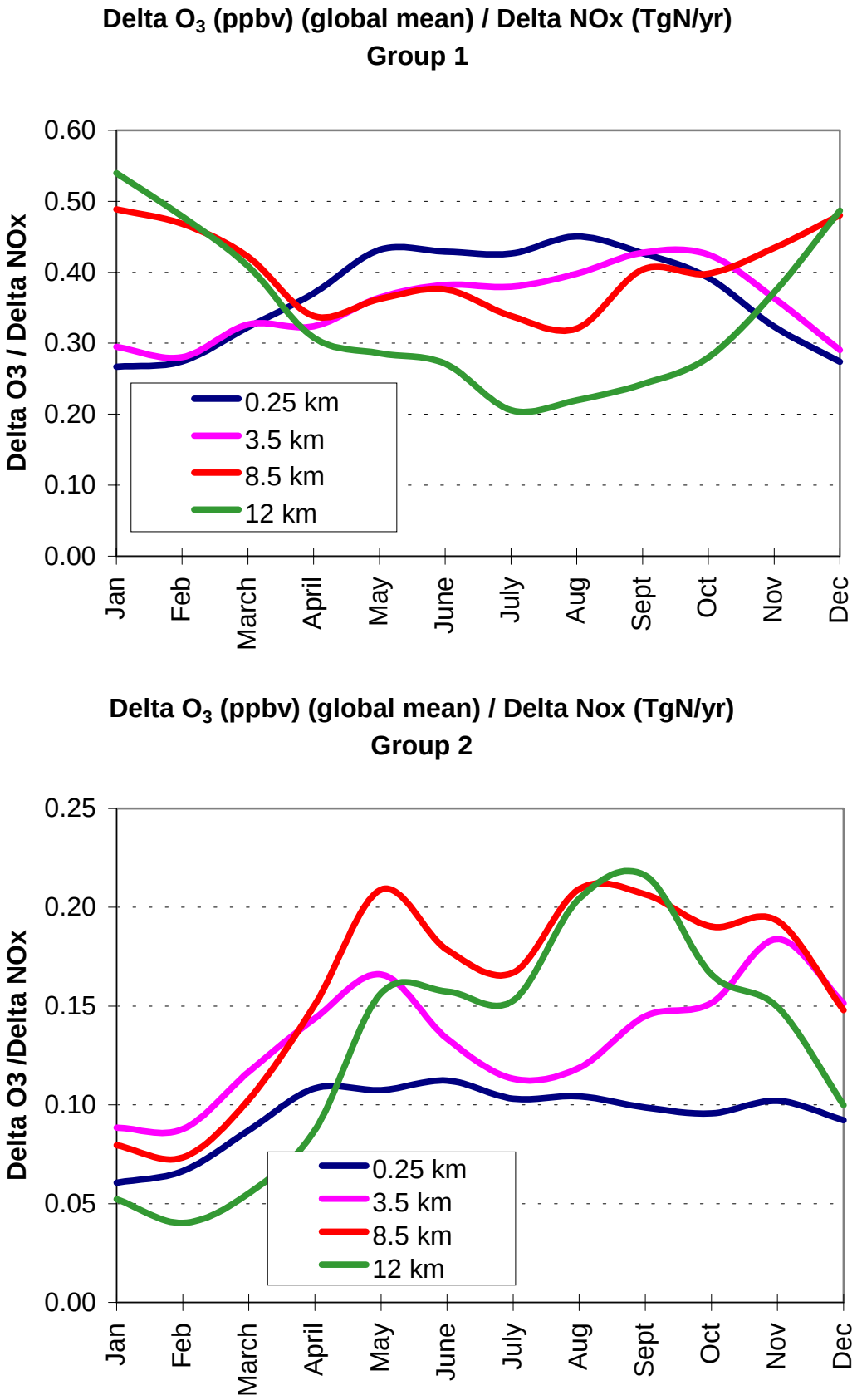

Figure 10. *Calculated O_3 change sensitivities (α) for the various groups and tests. Note different scales.*

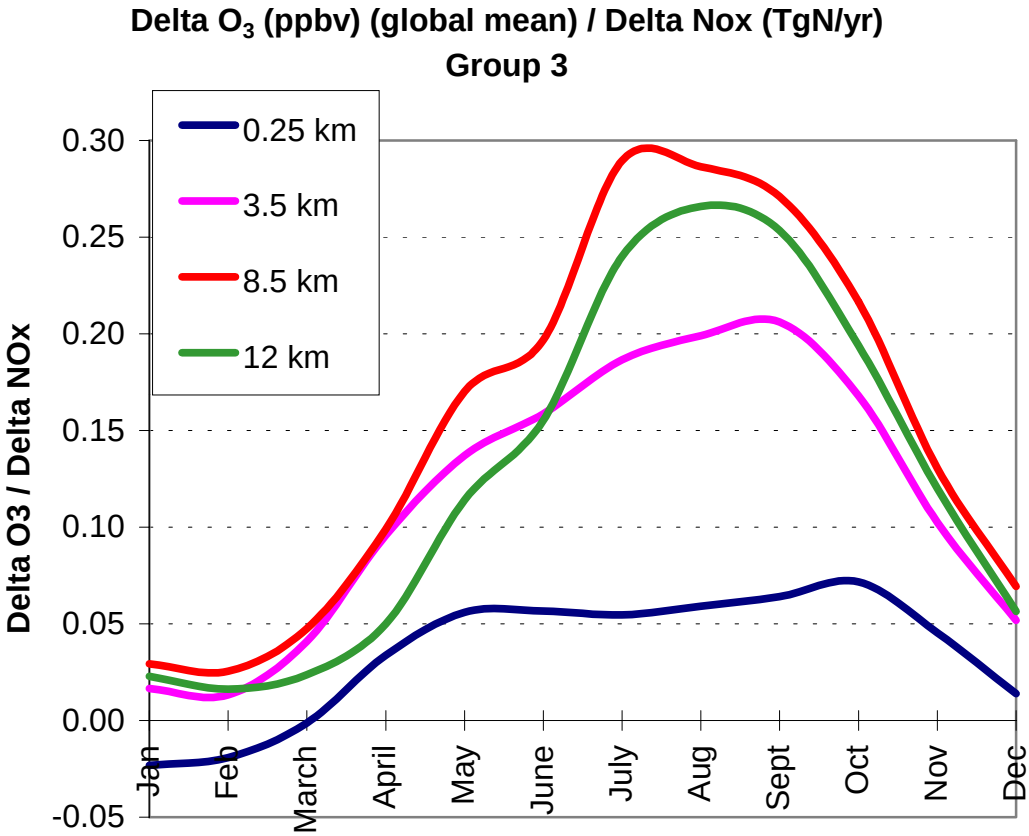

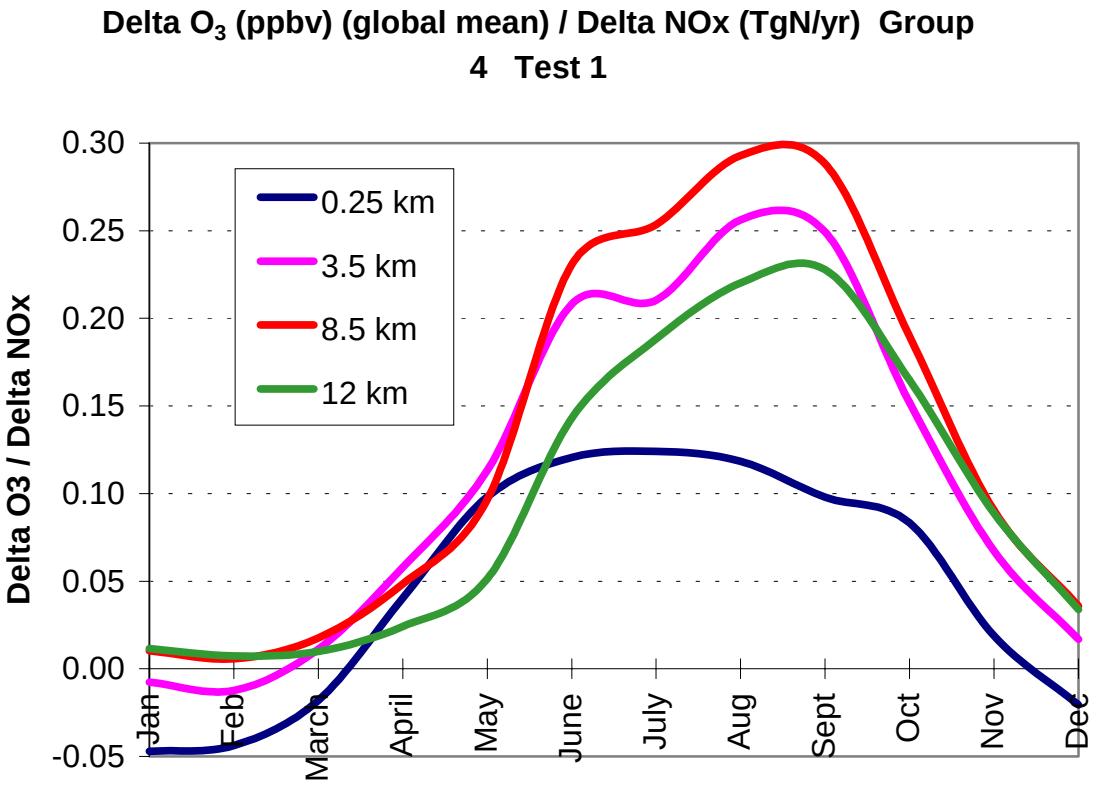

Figure 10. *(continued).*

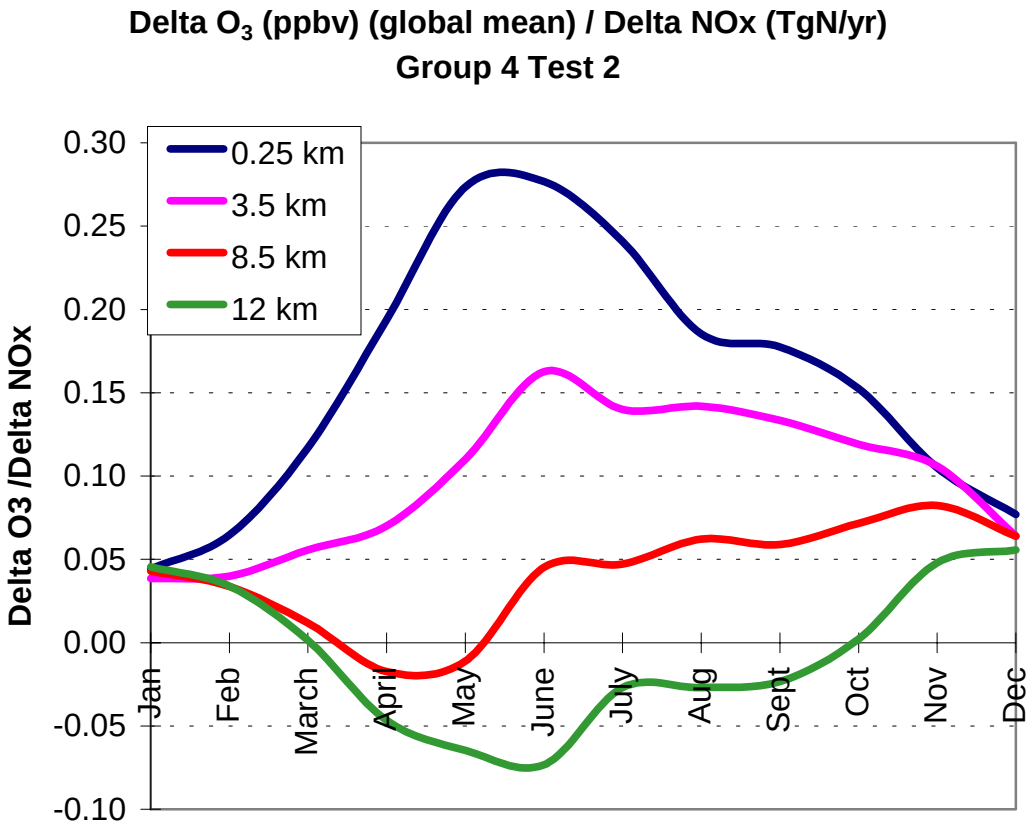

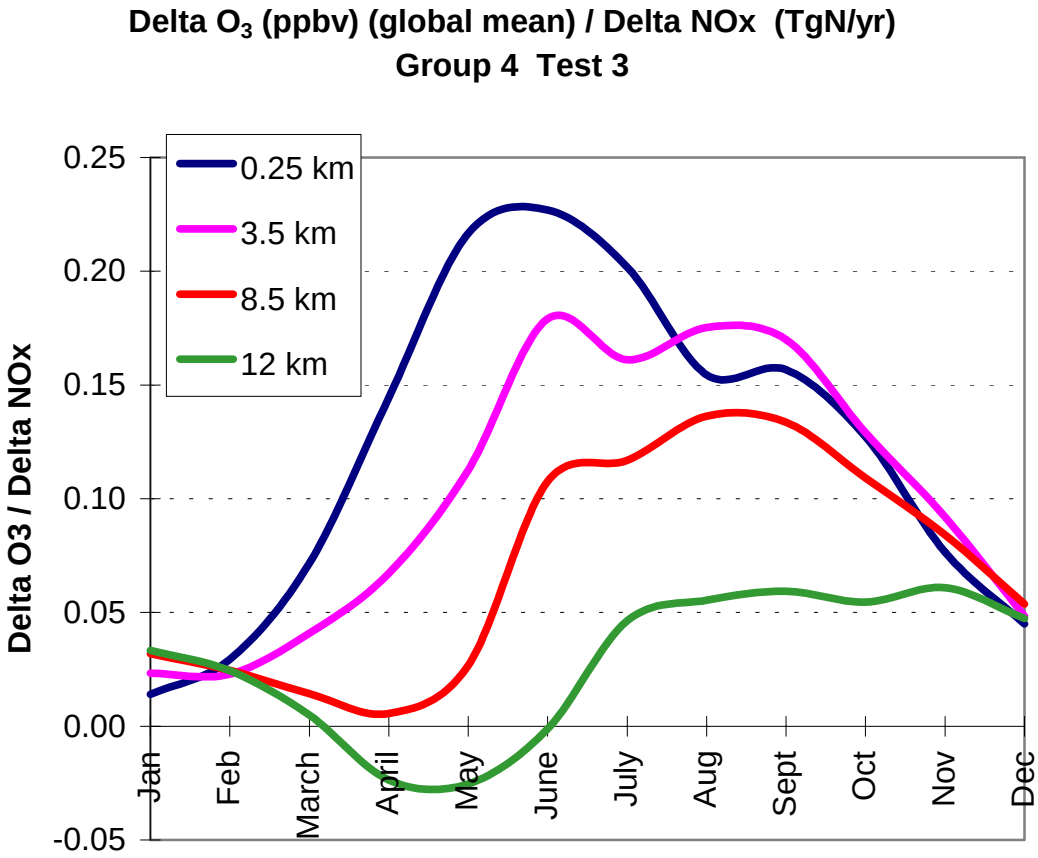

Figure 10. *(continued).*

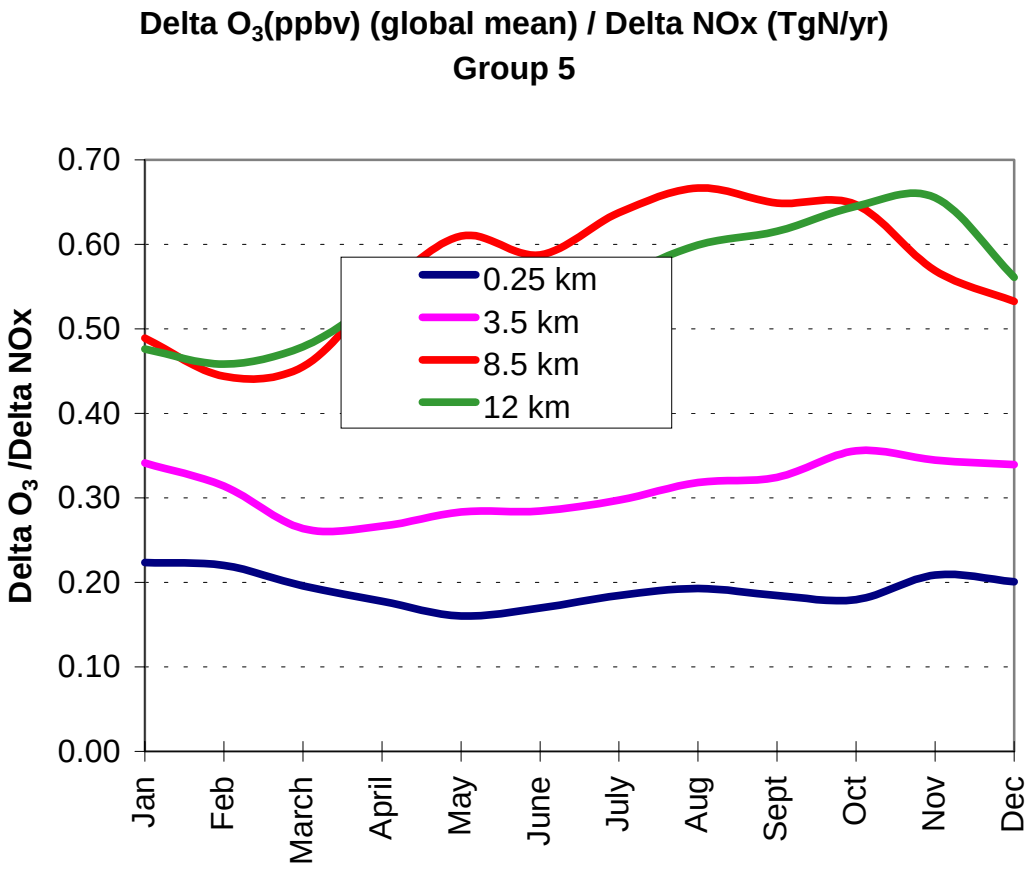

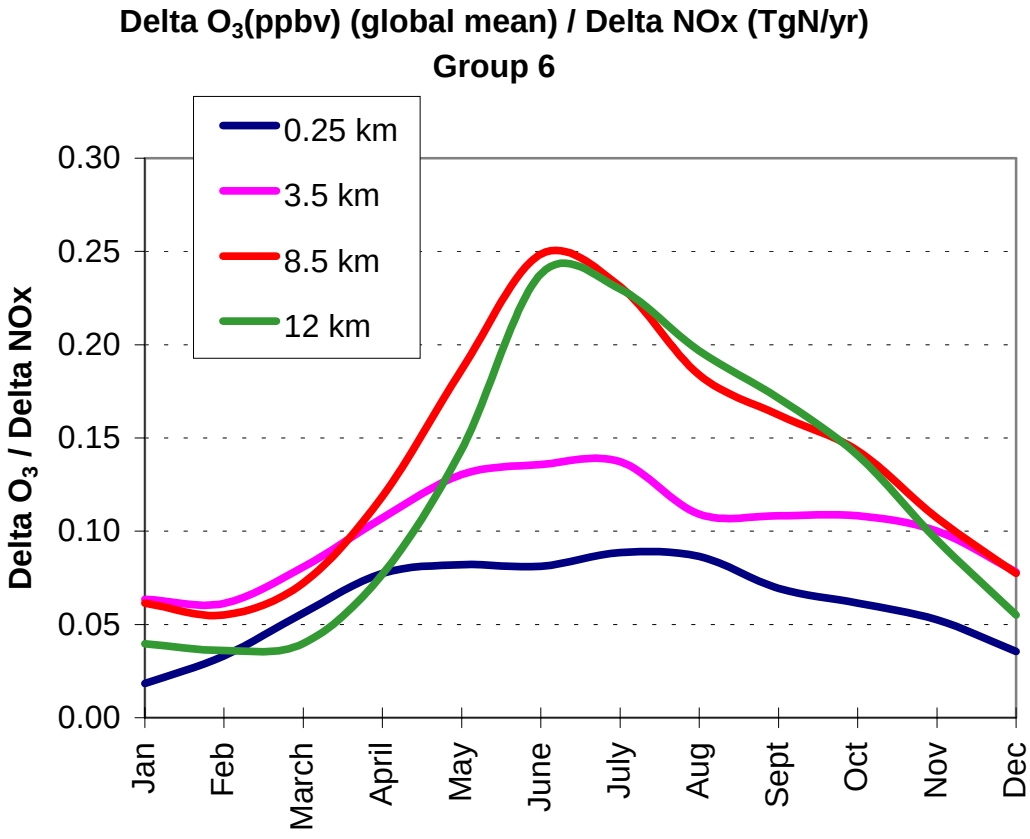

Figure 10 *(continued).*

The figures show that the highest sensitivities to NOx reductions are calculated for Southeast Asia and Australia, while USA and southern Europe have the lowest sensitivities. In contrast to the low latitude regions, the O_3 changes for regions at high latitudes show significant seasonal variation, particularly in the upper troposphere due to the stronger seasonal cycle in convective activity.

Ozone changes in the upper troposphere have the largest impacts on climate in terms of radiative forcing. Figure 11 shows the annual global change in ozone per change in NOx for 8.5 km and 12 km for the various regions. Again it is evident that the Southeast Asia has the largest sensitivity, followed bya Australia. Scandinavia, on the other hand, shows the lowest sensitivity.

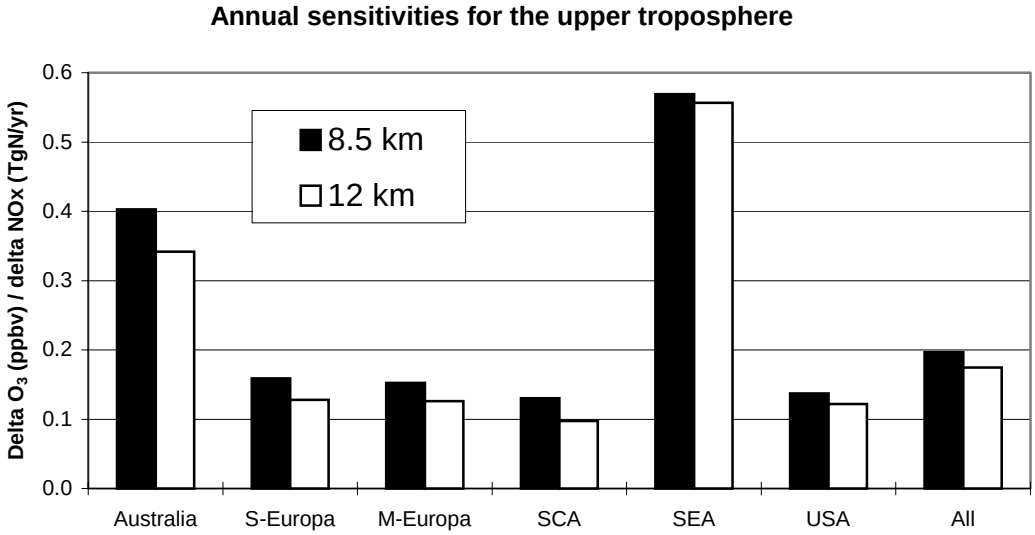

Figure 11. *Annual sensitivities for ozone changes for the upper troposphere.*

4.3 Changes in methane

Changes in NOx, CO and VOC emissions will not only affect ozone concentrations, but also the concentrations of OH. With respect to climate change, the primary effect of the changes in OH will be on methane. However, since the lifetime of methane is of the order of 10 years, 15 month simulations as performed in this project can not be used directly to estimate the effect on methane. This section describes the procedure applied to estimate the final effect on the methane concentrations at steady state.

The main loss mechanism for atmospheric methane is the reaction:

$$CH_4 + OH \rightarrow CH_3 + H_2O \qquad \text{R16}$$

This reaction is the starting point of a long chain of reactions which may compensate (or even overcompensate) the initial loss of OH (Crutzen, 1987; Berntsen et al., 1992).

When emissions of NOx to the atmosphere are changed the following sequence of events will take place:

$\Delta E_{NOx} \Rightarrow \Delta[OH]_0 \Rightarrow \Delta[CH_4]_0 \Rightarrow \Delta[OH] \Rightarrow \Delta[CH_4] \Rightarrow \Delta[OH] \Rightarrow$ etc.

The additional change in methane following the initial change in methane concentrations ($\Delta[CH_4]_0$), are referred to as the feedback effect.

In a 15 months model run only the first step in the sequence given above is calculated explicitly. However, it is only in this step that there will be significant non-linear response in the system and thereby large differences in the impact of NOx reductions in the different regions. When we consider the effect on methane concentrations, the parameter of primary interest is not really $\Delta[OH]_0$, but rather the change in lifetime of methane, given by equation 1 given below, which depends on the changes in OH.

The difference between the regions in the effect on methane caused by NOx reductions, is due to two factors: i) as discussed in the section 3.1, the changes in OH concentrations are very dependent on the absolute NOx concentration and ii) since the reaction rate between OH and methane is temperature dependent, OH changes in different regions will affect the lifetime of methane differently. The relative strength of the additional changes caused by the feedback effect will not be significantly different between the regions since the long lifetime of methane ensures that the initial change ($\Delta[CH_4]_0$) is uniformly distributed globally.

To show the differences between the regions we will start the discussion by examining the changes in the lifetime of methane following the initial change in OH concentrations ($\Delta[OH]_0$).

4.3.1 Initial changes in the lifetime of methane

Based on the modelled monthly mean concentrations of OH and methane and the temperature distribution in the CTM, changes in tropospheric mean lifetime of methane have been calculated by equation:

$$\tau = \left(\frac{\overline{k(T) \cdot OH(\lambda,\phi,z) \cdot CH_4(\lambda,\phi,z)}}{\overline{CH_4(\lambda,\phi,z)}} \right)^{-1} \qquad 1$$

where the reaction rate k is a function T, the temperature, which is function longitude (λ), latitude (ϕ), altitude (z) and time (5-day averaged temperatures are used in the CTM). $\overline{x}$ denotes tropospheric arithmetic mean of x. The calculated initial seasonal changes in the lifetime of methane, i.e. from the 15 months model run ($\Delta\tau_0 = \tau_0 - \tau_{ref}$, where τ_0 is the initial change in the lifetime for each region), are shown in figure 12 and annual averages in table 3. The largest impact on the lifetime is found for a 20% reduction of NOx-emission in the USA. However (see discussion in section 4.3.3), this is mainly due to the higher absolute change in the emissions for this region compared with the other regions.

Perturbation	ΔE_{NOx} (TgN/yr)	$\Delta\tau_0$ (years)
Gr1t1	-0.169	0.023
Gr2t1	-0.393	0.012
Gr3t1	-0.444	0.01
Gr4t1	-0.043	0.00106
Gr5t1	-0.236	0.035
Gr6t1	-1.506	0.048
All groups	-2.79	0.136
Gr4t2	-0.043	-0.0031
Gr4t3	-0.064	-0.0026

Table 3. *Absolute changes in NOx emissions due to a 20% reduction in the emissions in each group and the corresponding calculated initial changes in in lifetime of methane ($\Delta\tau_0$).*

The impact of reductions in VOC and CO emission (at least for Scandinavia, Gr4t2 and Gr4t3) is to offset the increase in lifetime caused by NOx reductions, as reactions with CO and VOCs constitute major loss reactions for OH.

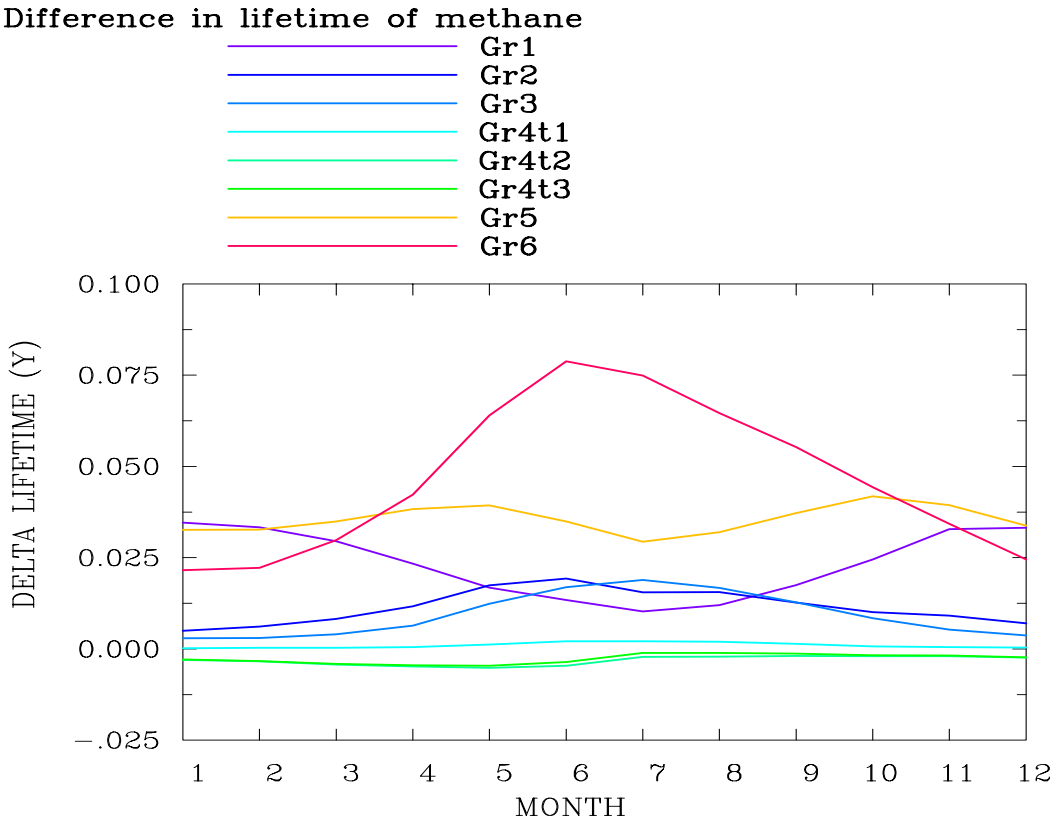

Figure 12. *Initial changes in the lifetime of CH_4 ($\Delta\tau_0$) in years given as function of month.*

In the following we will denote the concentrations of methane by C. The changes in methane concentrations, ΔC_0 (corresponding to $\Delta[CH_4]_0$), after the system has reached a new steady-state, but before the feedback effect is taken into account, can be calculated by the equation:

$$\Delta C_0 = C_{ref} \cdot \frac{\Delta \tau_0}{\tau_{ref}} \qquad 2$$

where τ_{ref} is the lifetime of methane in the reference run (8.14 years).

4.3.2 Total change in methane, including feedback

This initial change in methane concentration will then further influence the OH concentrations, giving a feedback effect on methane. The strength of this feedback is dependent on the magnitude of the initial perturbation (ΔC_0), and it is also model dependent mainly due to differences in the NOx distribution between models. In a work by Karlsdottir and Isaksen (1997), the same model as used in this work has been used to estimate the feedback strength by calculating the changes in the lifetime of methane following a 20% increase in methane concentrations. Assuming that the feedback strength does not vary significantly with the strength of the initial perturbation ($\Delta[CH_4]_0$), we can use the results from Karlsdottir and Isaksen (1997) to find a relation between a change in the methane concentration and a change in the lifetime (i.e. find Δ[OH]). The assumption described above is equivalent to the assumption that the ratio R, given in equation 3 is constant.

$$R = \frac{\Delta C / C}{\Delta \tau / \tau} \qquad 3$$

With a fixed ratio $\Delta C/C = 0.2$, Karlsdottir and Isaksen calculates a $\Delta\tau$ of approx. 7%, which gives a value of R of 2.85. We can then use this number to calculate an adjustment to the lifetime due to the feedback through the equation

$$R = \frac{\Delta C_0 \ / \ C_{ref}}{\Delta \tau_1 \ / \ \tau_{ref}} \qquad 4$$

Substituting for ΔC_0 from equation 2 then gives

$$\Delta \tau_1 = \Delta \tau_0 \ / \ R \qquad 5$$

This additional change in the methane concentration will lead to an additional feedback, further increasing the concentrations of methane. When we take into account these multiple feedback steps we can estimate the total change in the lifetime of methane due to both the initial perturbation following the reductions in the emissions and due to the feedback. The total change is given by the equation:

$$\Delta \tau = \Delta \tau_0 (1 + \sum_{n=1}^{\infty} \left(\frac{1}{R} \right)^n) \qquad 6$$

The convergent series $\sum_{n=1}^{\infty} \left(\frac{1}{R} \right)^n$ is equal to 0.54 when R = 2.85.

Total change in mean tropospheric steady-state concentration of methane can be calculated by:

$$\Delta C = C_{ref} \cdot \frac{\Delta \tau}{\tau} \qquad 7$$

The final change in global mean methane concentration, applying R = 2.85 is then given by

$$\Delta C = \Delta C_0 \cdot 1.54 \qquad 8$$

The final changes in methane concentrations are shown in table 5 (section 5.2).

When methane concentrations change due to changes in the emissions of methane there will be an effect on ozone (and thereby on OH and back on methane). In this study the change in methane concentrations is not caused by changes in emissions, and thus the number of methane molecules oxidized per unit of time remains the same. It is this latter quantity that mainly determines the ozone production potential. However, as the distribution of OH changes, there will be a small shift in the geographical and temporal distribution of the oxidation of methane, which in theory will have a small effect on the calculated changes in methane. To obtain a measure of this effect it is necessary to run each model experiment for several decades, which is not practically possible. Inclusion of this effect is considered negligible and is thus omitted.

4.3.3 Non-linear responses in methane

The perturbation performed by reducing NOx emissions by 20% in different regions shows significant non-linear behavior in the resulting change in the lifetime of methane. This is due to two factors: (i) difference in absolute magnitude of the perturbations and (ii) the differences in chemical environment of the regions. Especially will the background level of NOx be of great importance. To illustrate this effect we have calculated relative change in lifetime ($\Delta\tau_0$) with respect to emission change

$$\Delta \tau_{rel} = \frac{\Delta \tau_0}{\Delta E_{NO_x}} \qquad 8$$

where ΔE_{NOx} is the change in NOx-emissions for a given region in Tg(N)/yr.

Figure 13 shows the calculated seasonal variation in $\Delta\tau_{rel}$ for all the perturbations. Two regions, Australia (region 1) and Southeast Asia (region 5) stands out as being much more sensitive to changes in NOx emissions than the other regions. This is mainly due to the low background concentrations of NOx, and to a minor degree to the higher amounts of solar insolation in these regions due to their location at lower latitudes. The impact of the seasonal cycle in solar insolation is also evident for the other regions, giving the largest effects during summer in all regions.

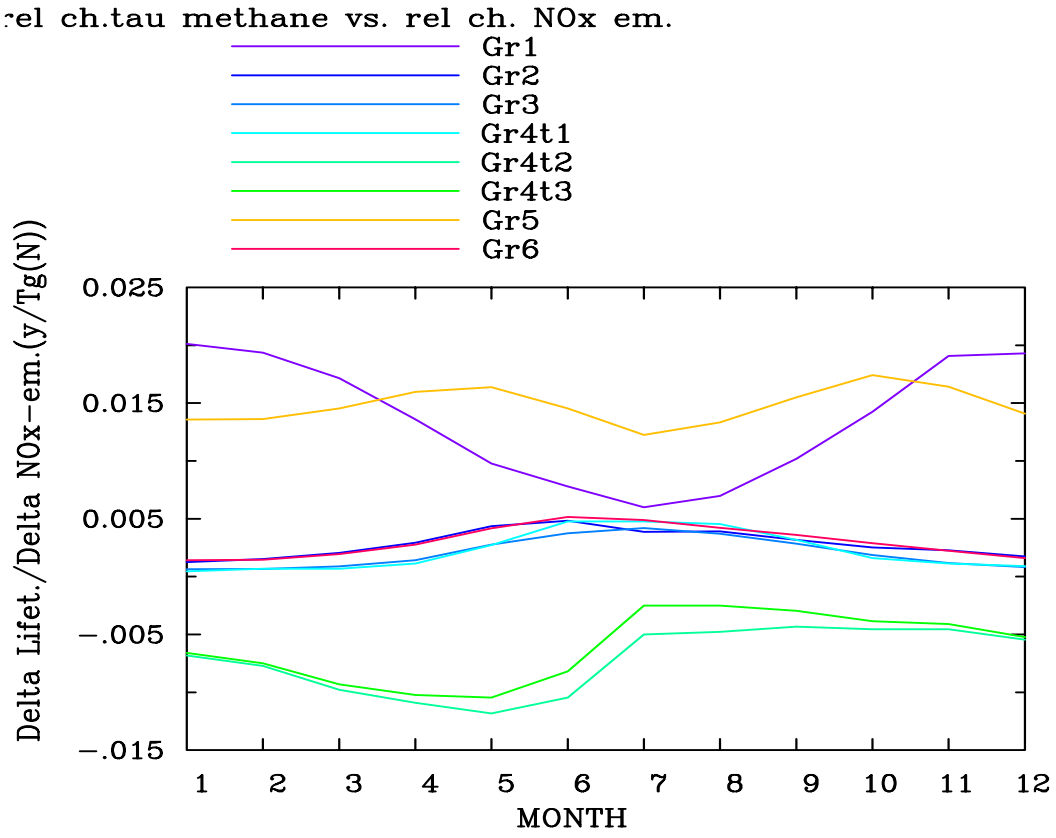

Figure 13. *Calculated seasonal variations in $\Delta\tau_{rel}$ (in years).*

5. Results from calculations of radiative forcing of climate

Due to transport in the atmosphere and the lifetimes of ozone and its precursors, the changes in ozone in response to changes in emissions will also occur over larger areas than only the region where the emission changes occur. This is especially the case for ozone in the upper troposphere due to the longer lifetime of O_3 (and NOx) in this region. Geographical averages of radiative forcing must therefore cover a much larger region than the region for the emission changes. Hemispheric averages are relevant in this context, but since group 5 is located at the equator changes in this group will affect both hemispheres. Global averages are therefore chosen for estimates of radiative forcing from ozone changes.

The change in the radiative balance of the Earth/atmosphere system is calculated as instantaneous forcing (i.e. no stratospheric temperature adjustment). Changes in tropospheric ozone leads to changes in the flux of longwave radiation to the lower stratosphere (and, to a much smaller extent, in the reflected shortwave radiation) which acts to cool the stratosphere. This affects the thermal infrared emission from the stratosphere which in turn affects the energy available for the surface-troposphere system. Since the temperature adjustments in the stratosphere take place on a time-scale of a few months, compared to the decadal time-scale of the surface temperature response, it is often considered to be part of the forcing. When the stratospheric temperature change is included, the forcing is called “adjusted”; otherwise it is referred to as “instantaneous”. As shown by Berntsen et al. (1996b), the neglect of adjustment may lead to an overestimate of between 20 and 30% in estimates of radiative forcing. In the present study, however, we focus on how the chemical changes and the radiative forcing varies between regions. Thus, since we are studying the relative differences, the neglect of stratospheric temperature adjustment is not critical for the conclusions.

Since methane has a lifetime long enough to permit homogeneous mixing in the atmosphere, we will only use the global mean mixing ratio in the calculations of radiative forcing from this gas.

5.1 Radiative forcing from changes in ozone

Table 4 shows the total (shortwave + longwave) radiative forcing in northern hemisphere (NH), southern hemisphere (SH) and for the whole globe for January, July as well as the annual global mean.

The radiative forcing due to 20% reduction of surface NOx emission is noticeable on a regional basis. But in terms of globally an annual averages the effects are negligible. However, if the radiative forcing is regionally heterogeneous, the impact on the dynamics of the atmosphere can be significant even for radiative forcing about one tenth of a W/m^2. The magnitude of radiative forcing is sensitive to the location of ozone change. In IPCC (1995), a few tenths W/m^2 of radiative forcing is considered significant. From this study, therefore, it can be seen that the effects of 20% reduction of surface NOx emission on radiative forcing are small global-wise, but on a regional basis, quite noticeable.

		NH	SH	GLOBAL
Southeast Asia	Jan	-0.439	-0.360	-0.400
	Jul	-0.432	-0.764	-0.598
	Annual	-0.522	-0.600	-0.561
USA	Jan	-0.324	-0.020	-0.171
	Jul	-1.963	-0.037	-1.000
	Annual	-1.021	-0.021	-0.521
Scandinavia	Jan	-0.001	0.000	-0.000
	Jul	-0.057	0.000	-0.028
	Annual	-0.025	0.000	-0.012
Scandinavia test 2	Jan	-0.007	-0.005	-0.006
	Jul	-0.006	-0.002	-0.004
	Annual	-0.006	-0.004	-0.005

Table 4. *Total radiative forcing (10^{-2} W/m^2) due to ozone changes for January and July for the different groups.*

For the regions USA and Southeast Asia, there are some outstanding characteristics. For both regions, the longwave radiative forcing dominates the total forcing. For example, the annual global mean total and longwave radiative forcing for USA are 0.005 and 0.004 W/m^2, respectively. There exists a strong seasonal variation in USA, reaching minimum in February and maximum in July. In Southeast Asia however, the seasonal variation in the changes is small. The radiative forcing is quite noticeable on the regional basis regardless of the small global values (see figures 14, 15 and 16). For instance, the magnitude can reach almost 0.1 W/m^2 along the east coast of USA in July. The distribution of radiative forcing shows that reduced emissions in USA mainly gives a forcing in the northern hemisphere. This is of course not the case for group 5 (Southeast Asia) situated at the equator.

Figure 14 and 15 show the calculated spatial distribution of ozone forcing for July and January for Southeast Asia and USA, respectively. Figure 16 shows the forcing for Scandinavia (test 1) for July. For January the forcing was negligible.

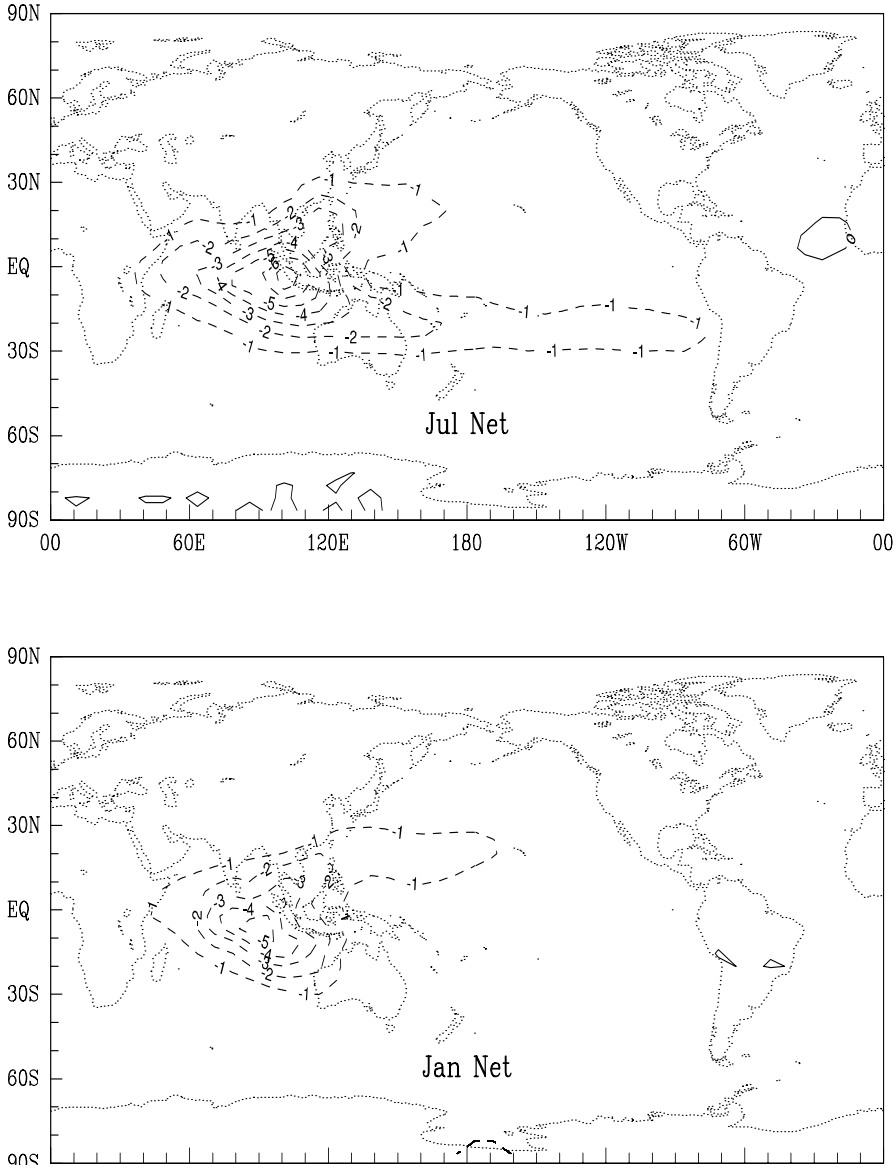

Figure 14. *Spatial distribution of total radiative forcing (shortwave + longwave) for January and July due to ozone changes in response to 20% reduction in NOx emissions in Southeast Asia (10^{-2} W/m^2).*

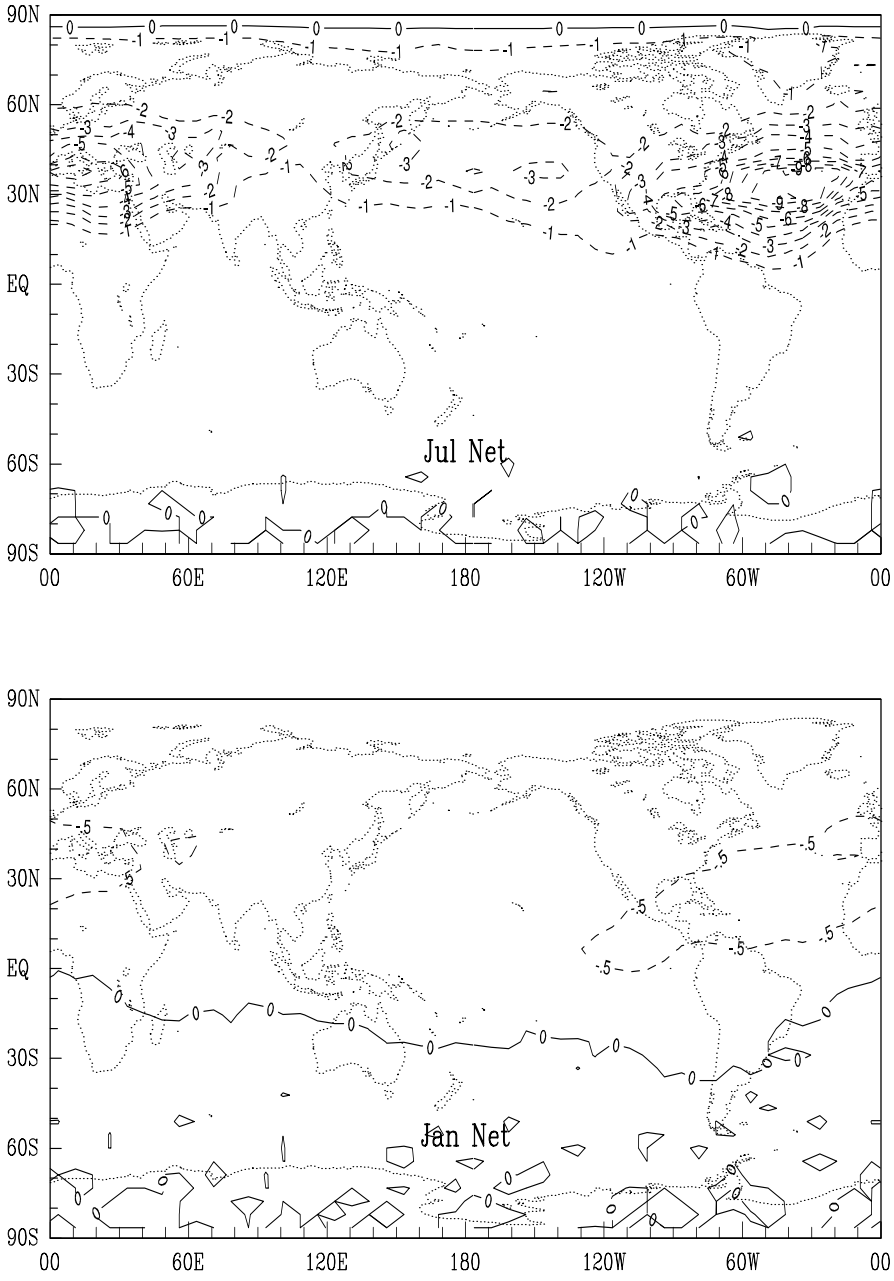

Figure 15. *Spatial distribution of total radiative forcing (shortwave + longwave) for January and July due to ozone changes in response to 20% reduction in NOx emissions in USA (10^{-2} W/m^2).*

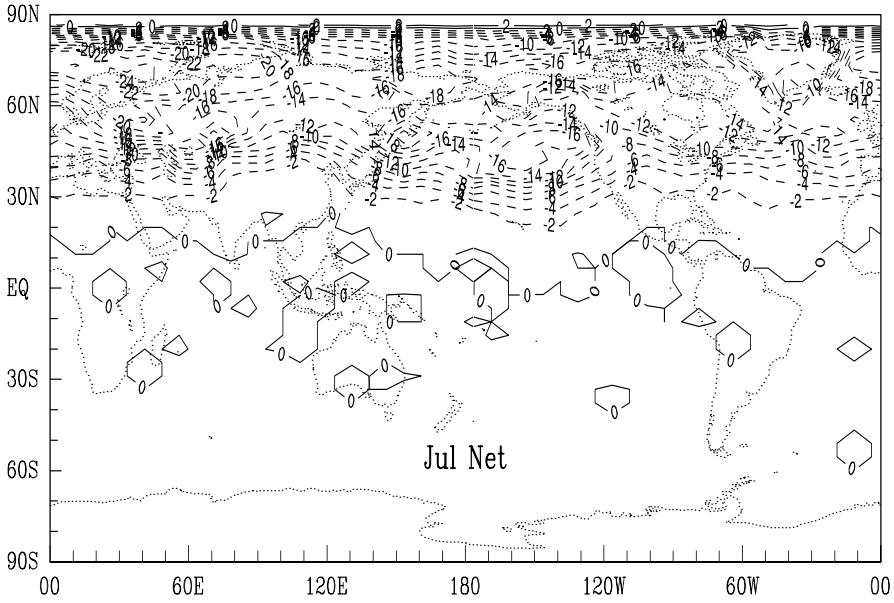

Figure 16. *Spatial distribution of total radiative forcing (shortwave + longwave) for July due to ozone changes in response to 20% reduction in NOx emissions in Scandinavia (10^{-4} W/m^2).*

Figure 17 and 18 shows the annual variation of global average radiative forcing from the calculated changes in ozone in the various regions. The figures show that the amplitude of the variation in the changes is larger for USA compared to Southeast Asia. They also show the smaller effect of reduced NOx emissions when VOC and CO emissions are reduced in addition, and that the reduction is occuring in the summer months.

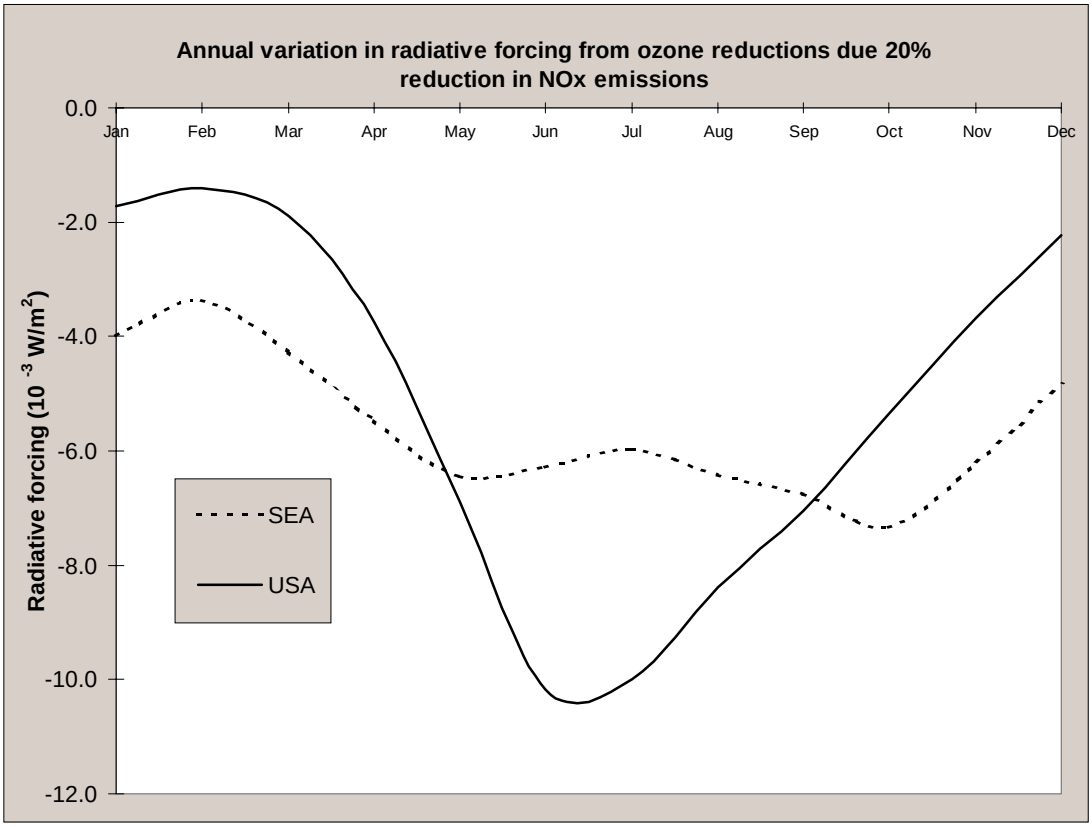

Figure 17. *Annual variation in global average radiative forcing from the calculated changes in ozone in response to 20% reduction in NOx emissions.*

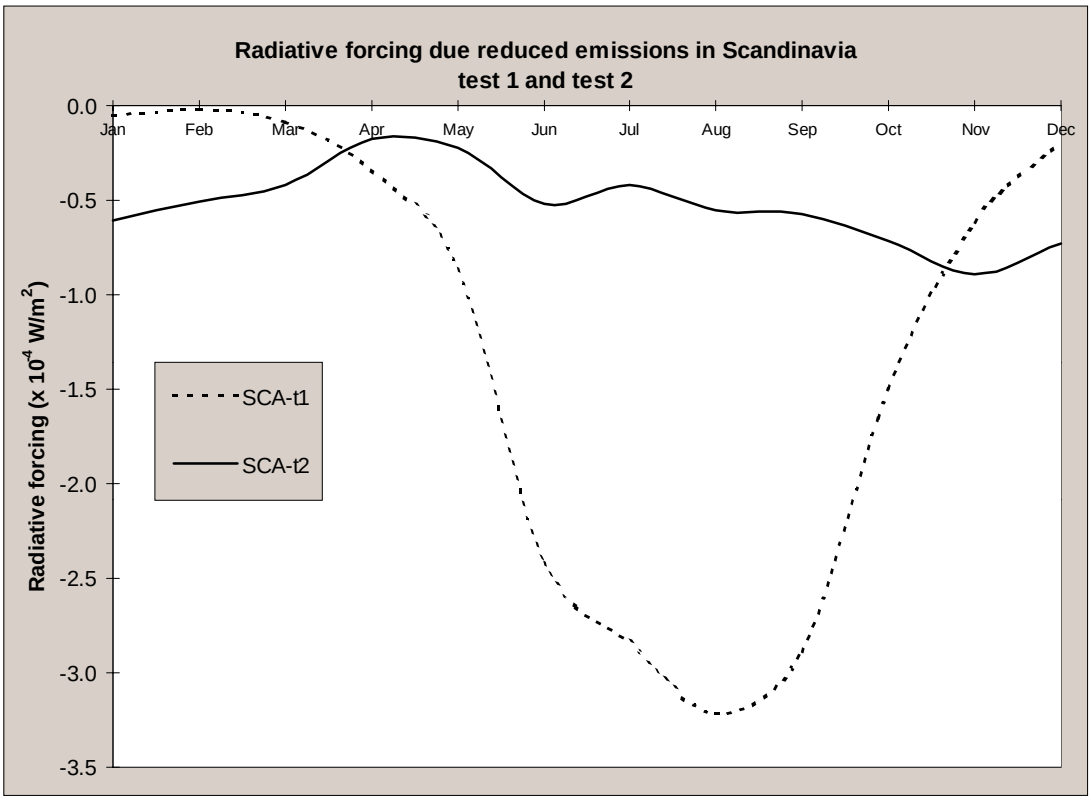

Figure 18. *Annual variation in global average radiative forcing from the calculated changes in ozone in response to 20% reduction in NOx emissions (test 1) and 30% reduction in CO and VOC in addition to the 20% reduction in NOx (test 2).*

5.2 Radiative forcing from changes in methane

Based on the changes in global mean concentrations of methane discussed in section 4.3, the radiative forcing can be calculated by the simple formula given in IPCC (1990)[2].

$$\Delta F = 0.036 \cdot (\sqrt{C_{ref} + \Delta C} - \sqrt{C_{ref}})$$

where C_{ref} is the global annual mean CH_4 mixing ratio (in ppbv).

The calculated total changes in methane and radiative forcing are given in table 5 for a 20% reduction in surface NOx sources. With regard to impact of emission changes of NOx in the different regions, the calculated radiative forcing is normalized to the absolute change in emission to give a sensitivity ratio for each region.

[2] In IPCC (1990) it is stated that the expression implicitly includes the radiative effects of global mean cloud cover. The calculations for methane forcing are thus consistent with the calculations for ozone.

Perturbation	ΔCH_4 (ppbv)	$\Delta F(CH_4)$ (10^{-2} W/m^2)	$\Delta F(CH_4)/\Delta E_{NOx}$ (10^{-2} W/m^2/TgN/yr)	$\Delta F(O_3)/\Delta E_{NOx}$ (10^{-2} W/m^2/TgN/yr)
Group 1, Australia	7.27	0.317	- 1.88	
Group 2, S-Europe	3.85	0.168	- 0.43	
Group 3, Central-Europe	3.22	0.141	- 0.32	
Group 4, Scandinavia	0.342	0.015	- 0.35	0.29
Group 5, Southeast Asia	11.5	0.501	- 2.12	2.37
Group 6, USA	15.7	0.684	- 0.45	0.35
All groups	43.8	1.9	- 0.68	0.60
Gr4t2	-1.01	-0.044		
Gr4t3	-0.846	-0.037		

Table 5. *Calculated total change in methane concentrations, radiative forcing and normalized radiative forcing for a 20% reduction in NOx emissions in 6 regions (Gr1t1-Gr6t1), and for two combined scenarios for Scandinavia (Gr4t2 and Gr4t3), which include VOC and CO reductions. The effect of 20% reduction simultaneously in all groups is also included.*

The table shows that radiative forcing per change in NOx emission through methane changes are largest for Southeast Asia and lowest for Central Europe and Scandinavia. Southeast Asia has also the highest sensitivity with respect to ozone forcing (se chapter 6).

6. Discussion and conclusions

The calculations show large variations between the regions in the *chemical* responses to changes in emissions (chapter 4). Focus has been given to impacts on the levels of ozone and methane in the troposphere. The responses in these gases vary significantly both with respect to *annual variation* of the changes as well as *magnitude* of the changes.

For ozone changes, the highest sensitivities to NOx reductions are calculated for Southeast Asia and Australia, while USA and Scandinavia have the lowest sensitivities. In contrast to the low latitude regions, the O_3 changes for regions at high latitudes show significant seasonal variation, particularly in the upper troposphere due to the seasonal cycle in convective activity.

For methane, two regions, Australia and Southeast Asia stand out as being much more sensitive to NOx changes than the other regions. Central Europe and Scandinavia show the lowest sensitivity to changes in NOx emissions.

The climatic impacts in terms of *radiative forcing* also shows significant regional variation. Due to spatial variations in climate parameters such as surface and tropospheric temperatures, cloud cover etc., even identical changes in ozone concentrations in different regions would not give equal radiative forcing. Changes in the concentrations of greenhouse gases will be particularly important in regions with few clouds and high surface temperature. Changes in climate gases that give a regionally heterogeneous radiative forcing will generally have larger impacts on climate than homogeneous changes with similar globally averaged radiative forcing. This is due to the physical processes that determines the circulation patterns in the atmosphere. The winds are driven by pressure gradients which are caused by heterogeneous heating of the surface and the atmosphere. Heterogeneous radiative forcing (as for ozone changes) will have stronger influence on the pattern of heating than homogeneous changes. Thus the circulation pattern is more likely to change causing larger climate changes in some regions and maybe less in others, if the radiative forcing is heterogeneous.

As shown in table 1 the magnitudes of the NOx emissions in the regions considered are very different. This is a consequence of the very different sizes of the regions, but technological and economical factors are also important. While the NOx emission in USA is 7.5 TgN/yr the emission in Scandinavia is only 0.2 TgN/yr. Since we have applied the same percentage reduction in all regions, the reductions in *absolute terms* are also very different. The changes in the concentrations of O_3 and CH_4 were therefore normalized to the magnitude of the emission reductions. The same is done for radiative forcing. Figure 19 shows the *annual variation of the normalized radiative forcing* for Southeast Asia, USA and Scandinavia (test 1 and 2).

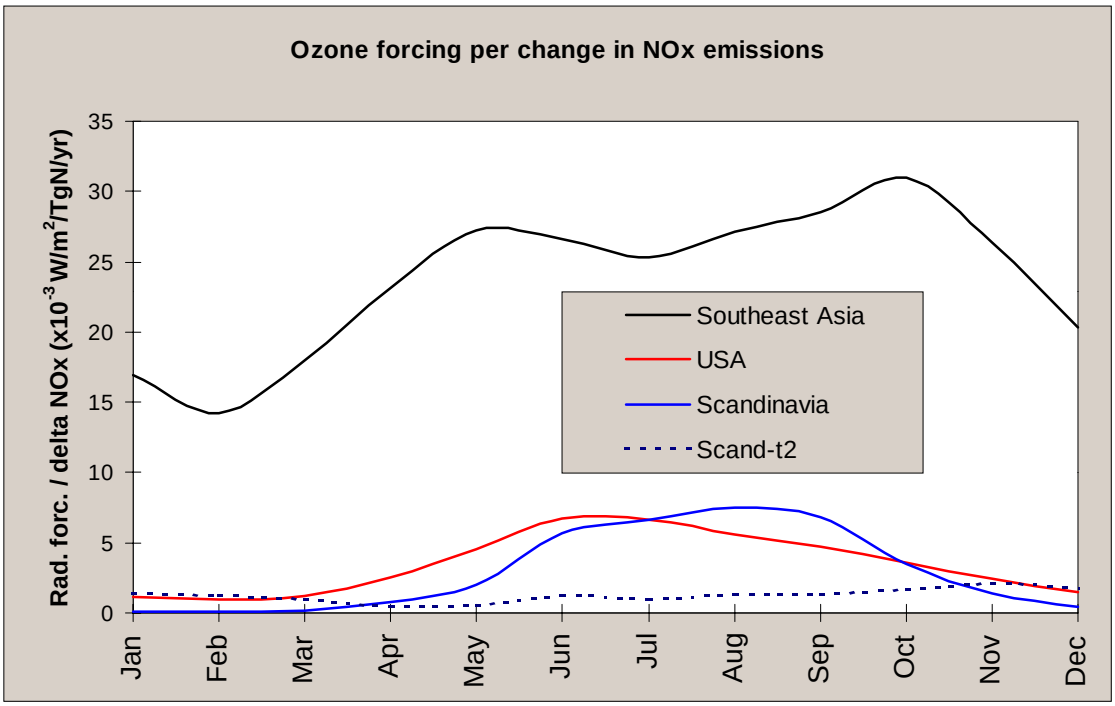

Figure 19. *Seasonal variation in the normalized ozone forcing.*

Significantly higher sensitivity in terms of radiative forcing to reductions in NOx emissions are found for Southeast Asia compared to the other regions. Differences in seasonal variations are also evident. On a per mass basis, the radiative forcing sensitivity to NOx changes are similar for USA and Scandinavia. As discussed earlier, the responses in O_3 to emission reductions in Scandinavia are lower when the emissions of VOC and CO also decrease. While figure 19 gives the seasonal variation in forcing per NOx change, figure 20 shows the *annual average forcing per NOx change*. Again the high sensitivity in Southeast Asia is evident, while USA and Scandinavia are on the same level. The sensitivity for Southeast Asia is larger than for Scandinavia by a factor of approximately 8, while the sensitivity for USA is approximately 20% larger than for Scandinavia.

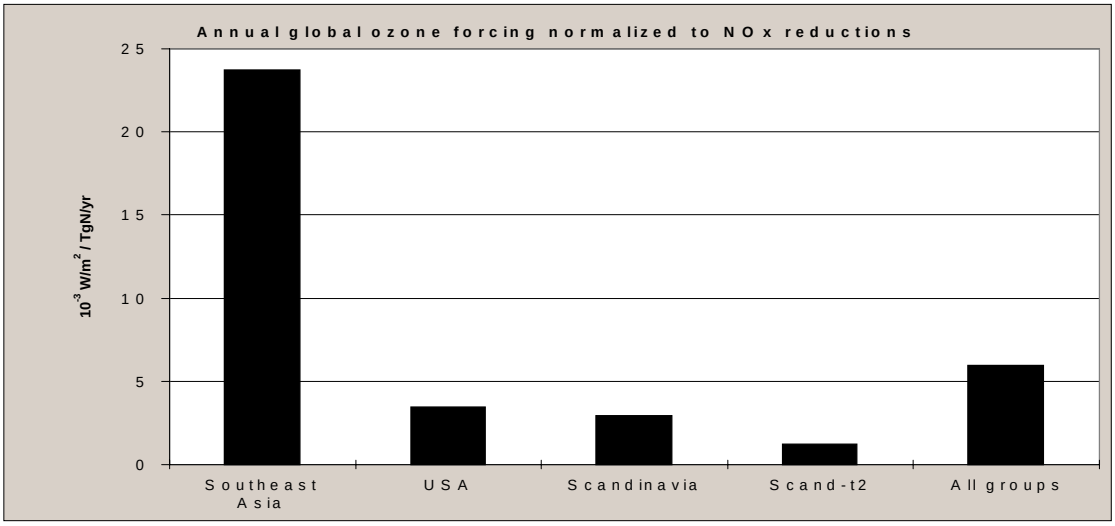

Figure 20. *Annual global ozone forcing for the different groups normalized to reductions in NOx.*

The maximum values for ozone forcing is also important to consider since the maximum radiative effect and the spatial gradients also are important for the dynamical response. The largest maximum ozone forcing is found for USA where the forcing reaches approximately -0.1 W/m^2 in July at 30°N and 40°W. For emission changes in Southeast Asia the forcing reaches approximately -0.09 W/m^2 at 10°S and 100°E in October. The maximum for Scandinavia is much smaller, approximately -0.0028 W/m^2 in August. (Note that these numbers are not normalized to the changes in NOx emissions).

For Scandinavia, three test were performed. In addition to the 20% reduction in NOx (test 1), two tests where the emissions of CO and VOC were reduced in addition to NOx. In test 2 the emissions of VOC and CO were reduced by 30% and NOx by 20%. In test 3 the emissions of NOx, VOC and CO were all reduced by 30%.

Test 2 and test 3 show very small differences for the boundary layer ozone concentrations compared to test 1. This underlines that VOC and CO concentrations in Scandinavia are less influenced by local sources than what is the case for NOx. In the upper free troposphere there are very pronounced differences between test 2/test 3 and test1. In test 2 and 3, ozone concentrations increase north of about 40°N during summer, while there is a decrease in the tropical regions. At the higher latitudes, which generally are NOx poor regions, the decreased amount of peroxy radicals (RO_2 and HO_2) produced through CO and VOC oxidation when VOC and CO are reduced, gives less chemical loss of ozone through the reactions between HOx and O_3, while in the tropical region the O_3 producing reactions are more important due to to higher NOx levels and stronger solar insolation. Figure 7 and 8 in Appendix 1, show that test 2 and 3 give roughly the same pictures of the changes in ozone. Further decreased NOx emissions in test 3 compared to test 2 cause an enhanced reduction of ozone as expected close to the source regions in Scandinavia. The reason for the difference at lower latitudes and in the southern hemisphere are more complex.

Due to the short lifetime of NOx, NOx concentrations at low latitudes in the northern hemisphere and in the southern hemisphere do not change much between test 2 and test 3. However, even if CO and VOC emissions are equal in test 2 and test 3 their concentrations at low latitudes and in the southern hemisphere are higher in test 2 compared to test 3. The unchanged NOx and higher CO and VOC concentrations in these regions in test 2 cause the slightly higher ozone concentrations. The reason for the increased CO and VOC concentrations at low latitudes and in the southern hemisphere is that the decrease in NOx and thus ozone and OH at higher latitudes increase the lifetime and enhance the southward transport of CO and VOC.

For test 2 the global annual radiative forcing was almost 60% lower than the forcing in the test with only NOx reductions (test 1). This reduction in forcing is strongly controlled by the changes in the upper troposphere. As shown in figure 10, the ozone reductions at 12 km are significantly smaller in test 2 than in test 1. The strong effect of changes in other gases on ozone and its radiative forcing points to the need for taking several gases into account in the formulation of reduction strategies. It also underlines the importance of modelling the background concentrations of other ozone precursors properly.

As shown in the chemistry calculations, changes in the emissions of NOx lead to changes in methane that are of opposite sign compared to the ozone response. As for ozone, there are regional variations in the response in methane to changes in NOx. This is due to the dependence of the OH chemistry to the existing NOx levels. Table 5 and figure 21 show the CH_4 response in terms of radiative forcing for the various groups normalized to the NOx change. The ratio between the forcing for Southeast Asia and for Scandinavia per change in emissions is approximately 6.

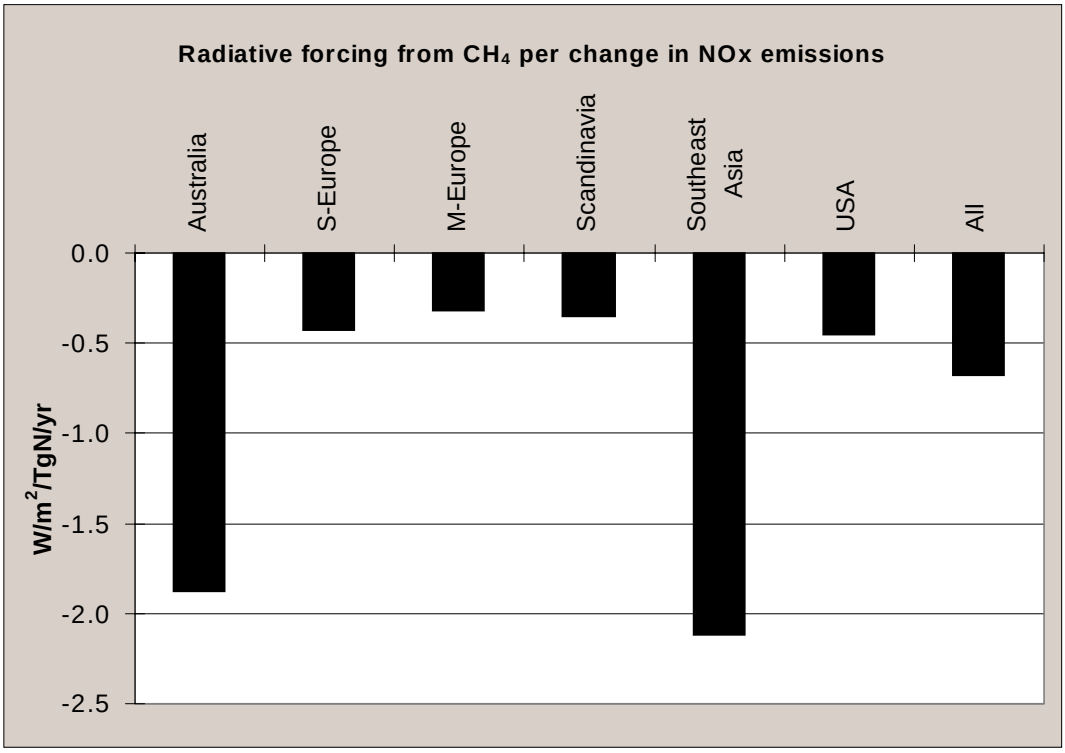

Figure 21. *Annual global methane forcing for the different groups normalized to reductions in NOx.*

Since the ozone and methane responses counteract each other it is of interest to compare the radiative forcing from these changes. Such comparisons are however hampered by the very different natures of these two responses. The radiative forcing from methane changes shows a quite homogenoeus global pattern while the ozone effect is much more regional, in spite of the longer lifetime at higher altitudes. In addition, due to the relatively long lifetime of methane, the response is delayed accordingly, while the ozone response is occuring during a few weeks. This fundamental differences in nature of climate forcing mechanism makes addition of the numbers for global mean radiative forcing (at steady state) somewhat dubious.

Figure 22 shows the global annual radiative forcing from changes in O_3 and CH_4 in response to 20% NOx reductions in the three regions USA, Southeast Asia and Scandinavia. In addition, the forcing is also given for the case with combined reductions in all groups. The effects in Southeast Asia and USA are of similar magnitudes (both the ozone and the methane effects), while the effects for Scandinavia are very small compared to the two other groups. For all groups, including the combinded case, the ozone forcing and the methane forcing are of similar magnitude, but of opposite sign. Due to the difficulties connected to addition of the ozone and methane effects, and the significant uncertainties connected to quantification of atmospheric relations, the *net* effect is not shown.

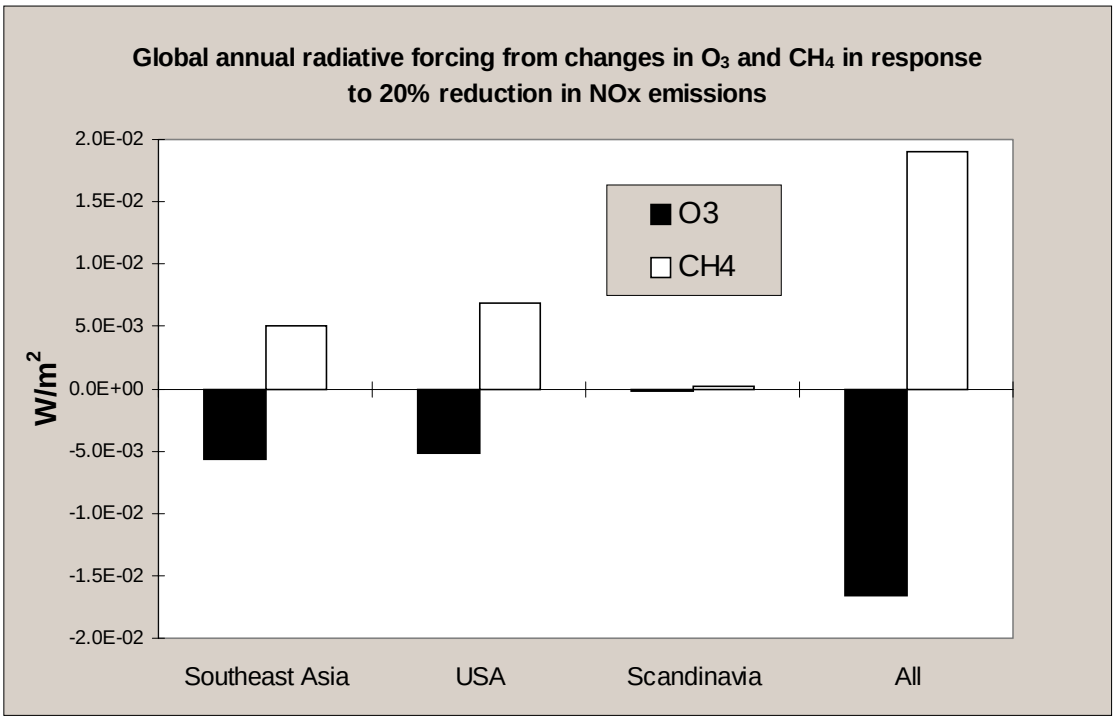

Figure 22. *Global annual forcing from changes in ozone and methane in response to 20% reduction in NOx emissions in Southeast Asia, USA and Scandinavia.*

If the numbers for annual forcing from methane and ozone normalized to the NOx changes in the regions, the picture is somewhat different, as shown in figure 23. In this perspective the emission reductions in Scandinavia and USA have the same radiative forcing per NOx reduction, while the sensitivity in Southeast Asia is significantly higher.

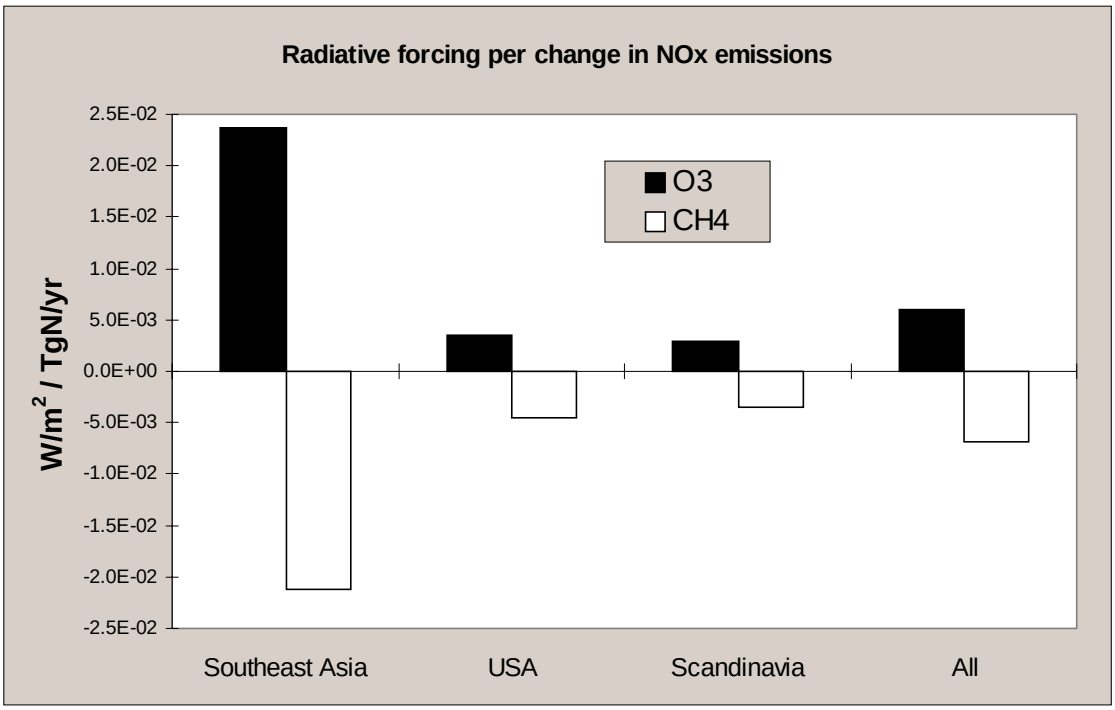

Figure 23. *Global annual forcing from changes in ozone and methane normalized to the reduction in NOx emissions in Southeast Asia, USA and Scandinavia.*

The calculations show that the chemical sensitivity is largest for Southeast Asia and Australia (figure 11). In addition to the differences in chemical responses between the regions, there are also variations in surface temperature and tropospheric temperature profile, clouds and water vapour levels, which will affect the forcing due to the changes in ozone.

The estimates of radiative forcing due to O_3 changes per change in NOx emissions ($Wm^{-2}/TgNyr^{-1}$) can be compared with other estimates in the litterature. For a 100% increase in global surface emissions of NOx, Hauglustaine et al. (1994b) calculate a sensitivity of $3.4 \cdot 10^{-3}$ $Wm^{-2}/TgNyr^{-1}$, while Fuglestvedt et al. (1996) calculate a forcing of $3.1 \cdot 10^{-3}$ $Wm^{-2}/TgNyr^{-1}$ for a 10% increase in global surface emissions. Both studies are peformed with 2-D models. In this 3-D study the estimated sensitivites for USA and Scandinavia are of similar magnitude, $3.46 \cdot 10^{-3}$ $Wm^{-2}/TgNyr^{-1}$ and $2.91 \cdot 10^{-3}$ $Wm^{-2}/TgNyr^{-1}$, respectively. Southeast Asia shows a much higher sensitivity, $2.38 \cdot 10^{-2}$ $Wm^{-2}/TgNyr^{-1}$. For CH_4, Fuglestvedt et al. (1996) calculate a forcing of approximately $-0.5 \cdot 10^{-2}$ $Wm^{-2}/TgNyr^{-1}$, while the numbers from this study are in the range -0.3 to $-2.1 \cdot 10^{-2}$ $Wm^{-2}/TgNyr^{-1}$. The opposing effects of ozone and methane responses are also found in several other studies, e.g. Lelieveld and Dorland (1995), Johnson and Derwent (1996), Hauglustaine et al. (1994b).

This study shows that emissions of NOx have potentially important impacts on climate. These impacts are, however, very different in nature; one global methane effect with a delay of approximately a decade, while the ozone effect is of regional character with an almost instaneous adjustment. Both mechanisms may affect climate on a hemispheric to global scale through changes in local heating rates and dynamics.

The study also shows that the effects of NOx emissions on ozone in the free troposphere depend on changes in the levels of gases providing the HOx precursors for ozone production. This is well known for surface ozone (e.g. Isaksen et al., 1978a,b). The effects depends therefore on how measures to reduce emissions affect the composition of the various emissions. Several source gases have common emission sources (NOx, CO, VOC) and measures implemented to reduce the emissions of one gas may also, depending on the nature of the measure) affect the emission of other gases.

Ackowledgements

This work has received support from the Norwegian State Pollution Control Authority and The Norwegian Research Council (to CICERO) and US National Science Foundation and US Department of Energy (to Atmospheric Sciences Research Center, State University of New York, Albany).

References

Berntsen, T., Fuglestvedt, J.S. and Isaksen, I.S.A. 1992. Chemical-dynamical modelling of the atmosphere with emphasis on the methane oxidation. *Ber. Bunsenges. Phys. Chem.*, 96, 241-251.

Berntsen, T. and Isaksen, I.S.A. 1994. A 3-D Photochemistry/transport model of the global troposphere. *Institute Report no. 89*. Department of Geophysics, University of Oslo.

Berntsen, T. 1994. Two- and three-dimensional model calculations of the photochemistry of the troposphere. *Dr. Scient. thesis*. Institute of Geophysics, University of Oslo.

Berntsen, T., Isaksen, I.S.A., Wang, W.-C. and Liang, X.-Z. 1996a. Impacts of increased anthropogenic sources in Asia on tropospheric ozone and climate: A global 3-D model study. *Tellus*, 48B, 13-32.

Berntsen, T., Isaksen, I.S.A., Fuglestvedt, J.S., Myhre, G., Stordal, F., Freckleton, R.S., and Shine, K.P., 1996b: Effects of anthropogenic emissions on tropospheric ozone and its radiative forcing. Submitted to *J. Geophys. Res.*

Berntsen T. and I.S.A. Isaksen. 1997. A global 3-D chemical transport model for the troposphere;1. Model description and CO and ozone results. Accepted for publication in *J. Geophys. Res*.

Crutzen, P.J. 1987. Role of the tropics in atmospheric chemistry. In: *The geophysiology of Amazonia*, Dickinson, R.E. (Ed.). John Wiley New York, 107-130.

Derwent, R. 1994. The estimation of Global Warming Potentials for a range of radiatively active gases. In: *Non-CO_2 Greenhouse gases: Why and how to control?*, Ham, J. van, Janssen, L.J.H.M., and Swart, R.J. (Eds.). Kluwer Academic Publishers, 289-299.

Dignon, J. 1992. NO_X and SO_X emissions from fossil fuels: a global distribution. *Atmos. Environ.*, 26A, 1157-1163.

Fuglestvedt, J.S., Berntsen, T.K and Isaksen, I.S.A. 1993. Responses in tropospheric O_3, OH and CH_4 to changed emissions of important trace gases. *Report 1993:4*. CICERO, May 1993.

Fuglestvedt, J.S., Jonson, J.E. and Isaksen, I.S.A. 1994. Effects of reductions in stratospheric ozone on tropospheric chemistry through changes in photolysis rates. *Tellus*, 46B, 172-192.

Fuglestvedt, J.S., Jonson, J.E., Wang, W.-C. and Isaksen, I.S.A. 1995. Responses in tropospheric chemistry to changes in UV fluxes, temperatures and water vapour densities. In: *Atmospheric Ozone as a Climate Gas*, Wang, W.-C. and Isaksen, I.S.A. (Eds.).

Fuglestvedt, J.S. 1995. Model studies of indirect effects on climate through changes in the chemistry of the troposphere. *Thesis for the degree Doctor Scientiarum*, Department of Chemistry, University of Oslo. CICERO, Oslo, 1995.

Fuglestvedt, J.S., Isaksen, I.S.A. and Wang, W.-C. 1996. Estimates of Indirect Global Warming Potentials for CH_4, CO and NO_X. *Climatic Change* 34, 405-437.

Hansen, J., Russell, G., Rind, D., Stone, P., Lacis, A., Lebedeff, S., Ruedy, R. and Travis, L. 1983. Efficient three dimensional global models for climate studies: Models I and II. *Mon. Weather Rev.*, 111, 609-662.

Hauglustaine, D.A., Granier, C., Brasseur, G.P. and Mégie, G. 1994a. The importance of atmospheric chemistry in the calculation of radiative forcing of the climate system. *J. Geophys. Res.*, 99, 1173-1186.

Hauglustaine, D.A., Granier, C., Brasseur, G.P. and Mégie, G. 1994b. Impact of present aircraft emissions of nitrogen oxides on tropospheric ozone and climate forcing. *Geophys. Res. Lett*, 21, 2031-2034.

Hertel, O., Berkowicks, R., Christensen, J. and Hov, Ø. 1993. Test of two numerical schemes for use in atmospheric transport-chemistry models. *Atmos. Environ.*, 27A, 2591-2611.

Hesstvedt, E., Hov, Ø. and Isaksen, I.S.A. 1978. Quasi steady-state approximation in air pollution modelling: Comparison of two numerical schemes for oxidant prediction. *Int. J. Chem. Kin*., 10971-10994.

Hough, A.M. 1991. Development of a two-dimensional tropospheric model. Model chemistry. *J. Geophys. Res.*, 96, 7325-7362.

Intergovernmental Panel on Climate Change (IPCC) 1990. *Climate change. The IPCC Scientific Assessment*, Houghton, J.T., Jenkins, G.J. and Ephraums, J.J. (Eds.). Cambridge University Press, Cambridge, U.K.

Intergovernmental Panel on Climate Change (IPCC) 1992. *Climate change 1992. The Supplementary Report to The IPCC Scientific Assessment*, Houghton, J.T., Callander, B.A. and Varney, S.K. (Eds.). Cambrigde University Press, Cambridge, U.K.

Intergovernmental Panel on Climate Change (IPCC) 1994. *Radiative forcing of Climate change*. The 1994 Report of the Scientific Assessment Working group of IPCC. Summary for Policymakers.

Intergovernmental Panel on Climate Change (IPPC) 1995. *Climate Change 1995: The Science of Climate Change.* Cambridge University Press, Cambridge, U.K.

Isaksen, I.S.A., Midtbø, K.H., Sunde, J. and Crutzen, P.J. 1977. A simplified method to include molecular scattering and reflection in calculation of photon fluxes and photodissociation rates. *Geophys. Norv.*, 31, 11-26.

Isaksen, I.S.A., Hesstvedt, E. and Hov, Ø. 1978a. A chemical model for urban plumes: Test for ozone and particulate sulfur formation in St. Louis urban plume. *Atmos. Environ.*, 12, 599-604.

Isaksen, I.S.A., Hov, Ø. and Hesstvedt, E. 1978b. Ozone generation over rural areas. *Envir. Sci. Tech.*, 12, 1279-1284.

Isaksen, I.S.A. 1980. The tropospheric ozone budget and possible man-made effects. In: *Proceedings of the Quadrennial International Ozone Symposium*, Vol II., London, J. (Ed.). International Ozone Commission, Boulder, CO, Aug. 1980, 845-852.

Isaksen, I.S.A. and Hov, Ø. 1987. Calculations of trends in the tropospheric concentrations of O_3, OH, CO, CH_4 and NO_X. *Tellus*, 39B, 271-283.

Isaksen, I.S.A., Lee, Y.-P., Atkinson, R., Sidebottom, H., Fuglestvedt, J.S., Johnson, C., Lelieveld, J. and Thompson, A. 1992. Chapter 5: Tropospheric processes: Observations and interpretation. In: *Scientific Assessment of Ozone Depletion: 1991*, World Meteorological Organization, Global Ozone Research and Monitoring Project, Report No. 25, 1992.

Johnson, C.E. 1994. Global Warming from aircraft NOx emissions. In proceedings from *International Scientific Coloqium on the impact of emissions from aircraft and spacecraft upon the atmosphere*.

Johnson, C.E. and Derwent, R.G. 1996. Relative Radiative Forcing Consequences of Global Emissions of Hydrocarbons, Carbon Monoxide and NOx from Human Activities Estimated a Zonally-averaged Two-dimensional Model. *Climatic Change* 34, 439-462.

Jonson, J.E. and Isaksen, I.S.A. 1991. The impact of solar flux variations on the tropospheric ozone chemistry. *Institute Report no. 81*. Institute of Geophysics, University of Oslo.

Karlsdottir, S. and Isaksen, I.S.A. 1997. Feedback calculations of methane; a 3-D model study. In prep.

Lacis, A.A., Wuebbles, D.J. and Logan, J.A. 1990. Radiative forcing of climate by changes in the vertical distribution of ozone. *J. Geophys. Res.*, 95, 9971-9981.

Lelieveld, J., Crutzen, P.J. and Rodhe, H. 1989. Zonal average cloud characteristics for global atmospheric chemistry modelling. *Report CM 76*, UDC 551.510.4 Dep. of Meteorology, University of Stockholm, International Meteorological Institute in Stockholm.

Lelieveld, J. and van Dorland, R. 1995. Ozone Chemistry changes in the troposphere and consequent radiative forcing of climate. In: Atmospheric Ozone as a Climate Gas. Wang, W.-C. and Isaksen, I.S.A. (eds). NATO ASI series, Springer-Verlag Co., Heidelberg

Lin, X., Trainer M. and Liu S.C. 1988. On the nonlinearity of the tropospheric ozone production. *J. Geophys. Res.*, 93, 15879-15888.

Liu, S.C., Trainer M., Fehsenfeld F.C., Parrish D.D., Williams E.J., Fahey G. Hübler D.W. and Murphy, P.C. 1987. Ozone production in the rural troposphere and the implications for regional and global ozone distributions. *J. Geophys. Res.*, 92, 4191-4207.

Marenco, A., Gouget, H., Nédelec, P., Pagès, J.-P. and Karcher, F. 1994. Evidence of a long-term increase in tropospheric ozone from Pic du Midi data series-consequences: positive radiative forcing. *J. Geophys. Res.*, 99, 16617-16632.

Pickering, K., Thompson, A. M., Scala, J.R., Tao, W.-K., Dickson, R.R. and Simpson, J. 1992. Free troposphere ozone production following entrainment of urban plumes into deep convection. *J. Geophys. Res.*, 91, 17985-18000.

Poppe, D., Wallasch, M. and Zimmermann, J. 1993. The dependence of the concentrations of OH on its precursors under moderatly polluted conditions. A model study. *J. Atmos. Chem.*, 16, 61-78.

Prather, M., 1986. Numerical advection by conservation of second-order moments. *J. Geophys. Res.*, 91, 61-78.

Prather, M., McElroy, M., Wofsy, S., Russel, G. and Rind, D. 1987. Chemistry of the global troposphere: fluorocarbons as tracers of air motion. *J. Geophys. Res.*, 92, 6579-6613.

Russell, G.L. and Lerner, J.A. 1981. A new finite differencing scheme for the transport equation. *J. Appl. Meterorol.*, 20, 1483-1498.

Thompson, S.L. and Polland. 1995. A global climate model (GENESIS) with a land-surface-transfer scheme (LSX). Part 1: Present-day climate. *J. Climate*, 8, 732-761.

Wang, W.-C., Pinto, J.P. and Yung, Y.L. 1980. Climatic effects due to halogenated compounds in the earth's atmosphere. *J. Atmos. Sci*., 37, 333-338.

Wang, W.-C., Zhuang, Y.-C. and Bojkov, R.D. 1993. Climate implications of observed changes in ozone vertical distributions at middle and high latitudes of the Northern Hemisphere. *Geophys. Res. Lett.*, 20, 1567-1570.

Wang, W.-C., Liang, X.-Z., Dudek, M.P., Polland, D.D. and Thompson, S.L., 1995: Atmospheric ozone as a climate gas. *Atmos. Res.*, 37, 247-256.

Watson J.J., J.A. Probert, S.D. Piccot, J.W. Jones, 1991. Global inventory of volatile organic compound emissions from anthropogenic sources. EPA-report EPA-600/8-91-002.

APPENDIX 1

Figures showing calculated changes in ozone (%) for June ane December in the lowest layer (L=1) and for 12 km (L=7).

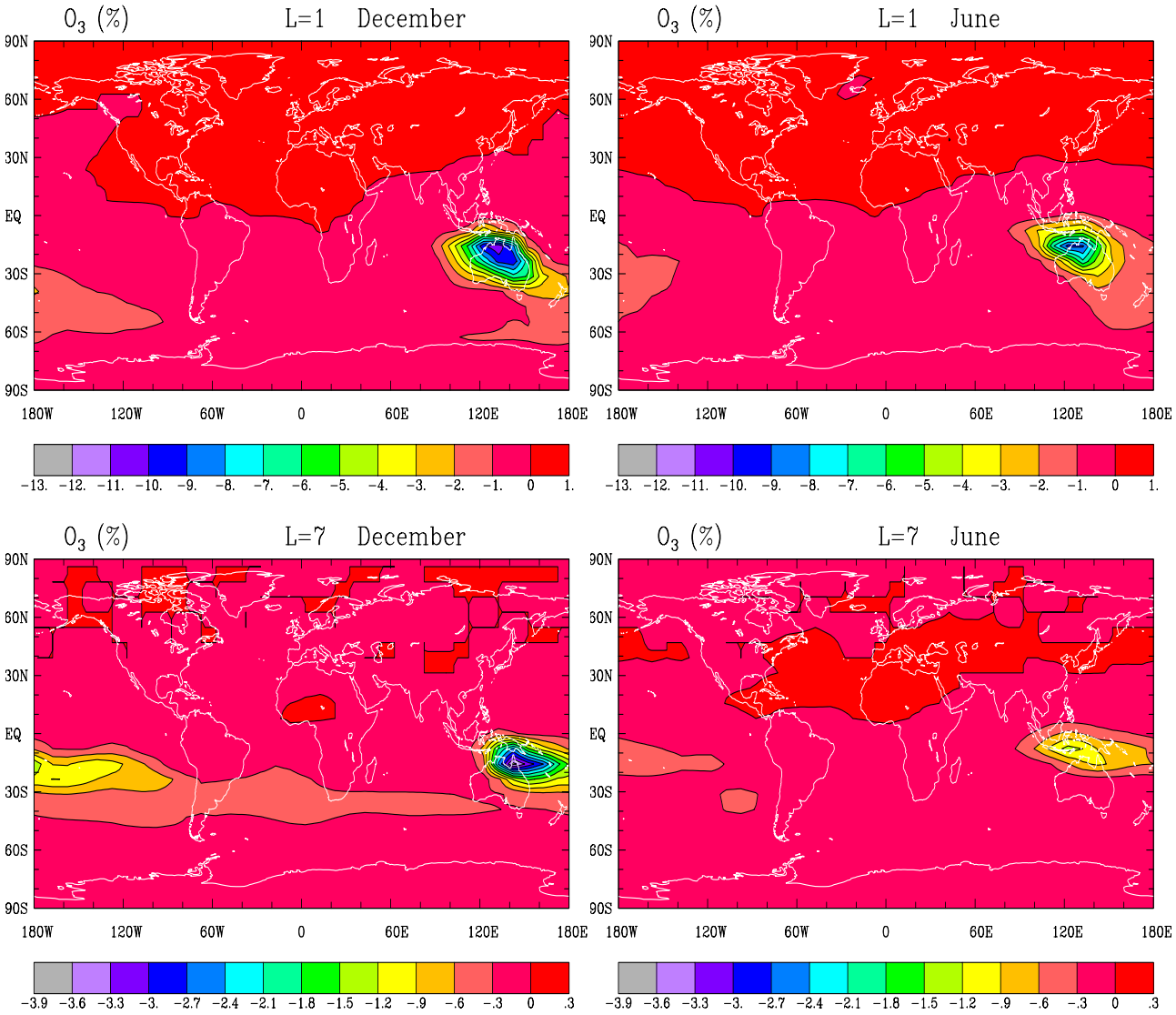

Figure 1: Calculated percentage change in the volume mixing ratio ozone for group 1 (Australia) at the surface (L=1), and in the upper free troposphere (L=7, approx. 12 km altitude) for December and June.

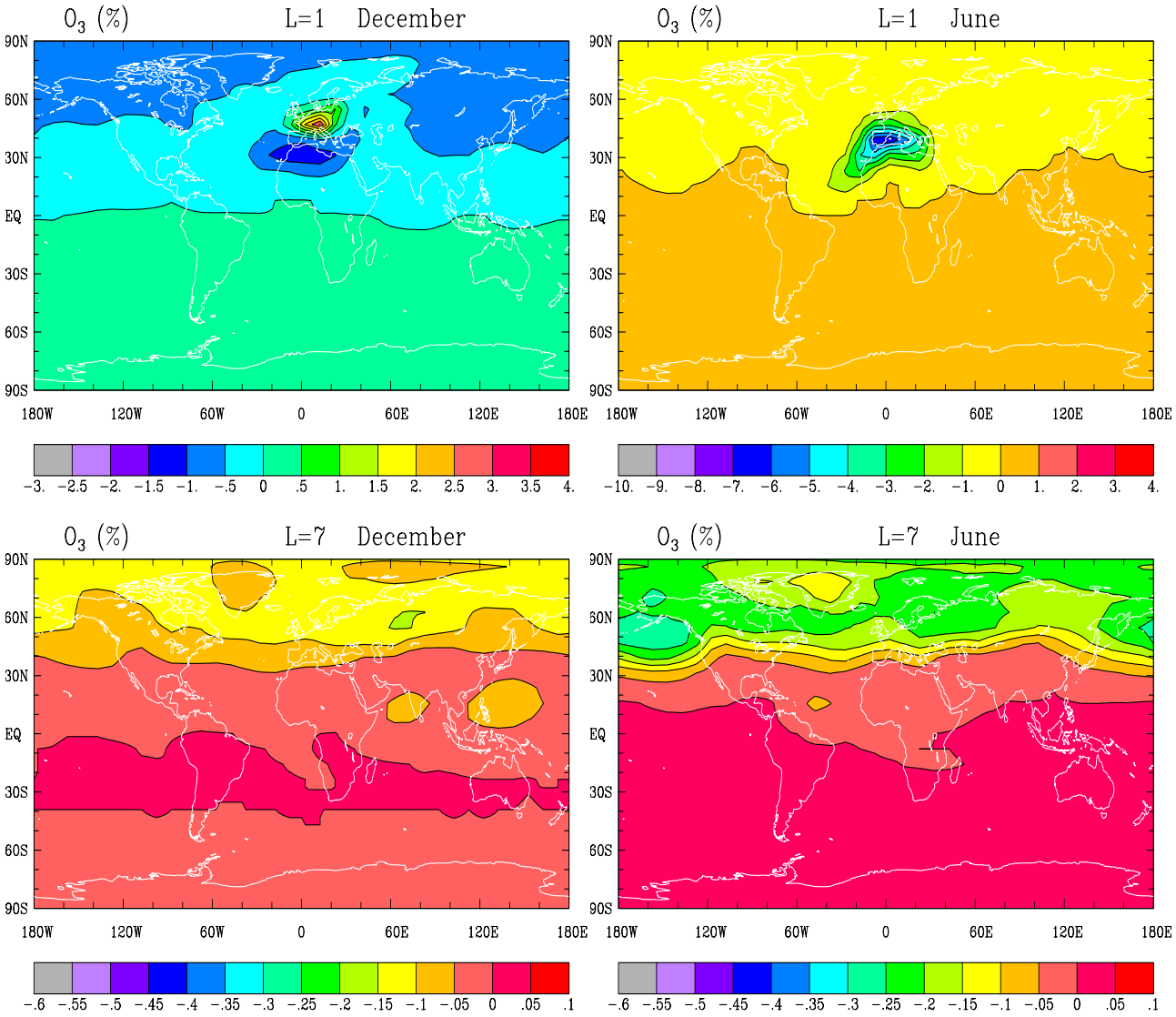

Figure 2: Calculated percentage change in the volume mixing ratio ozone for group 2 (Southern Europe) at the surface (L=1), and in the upper free troposphere (L=7, approx. 12 km altitude) for December and June.

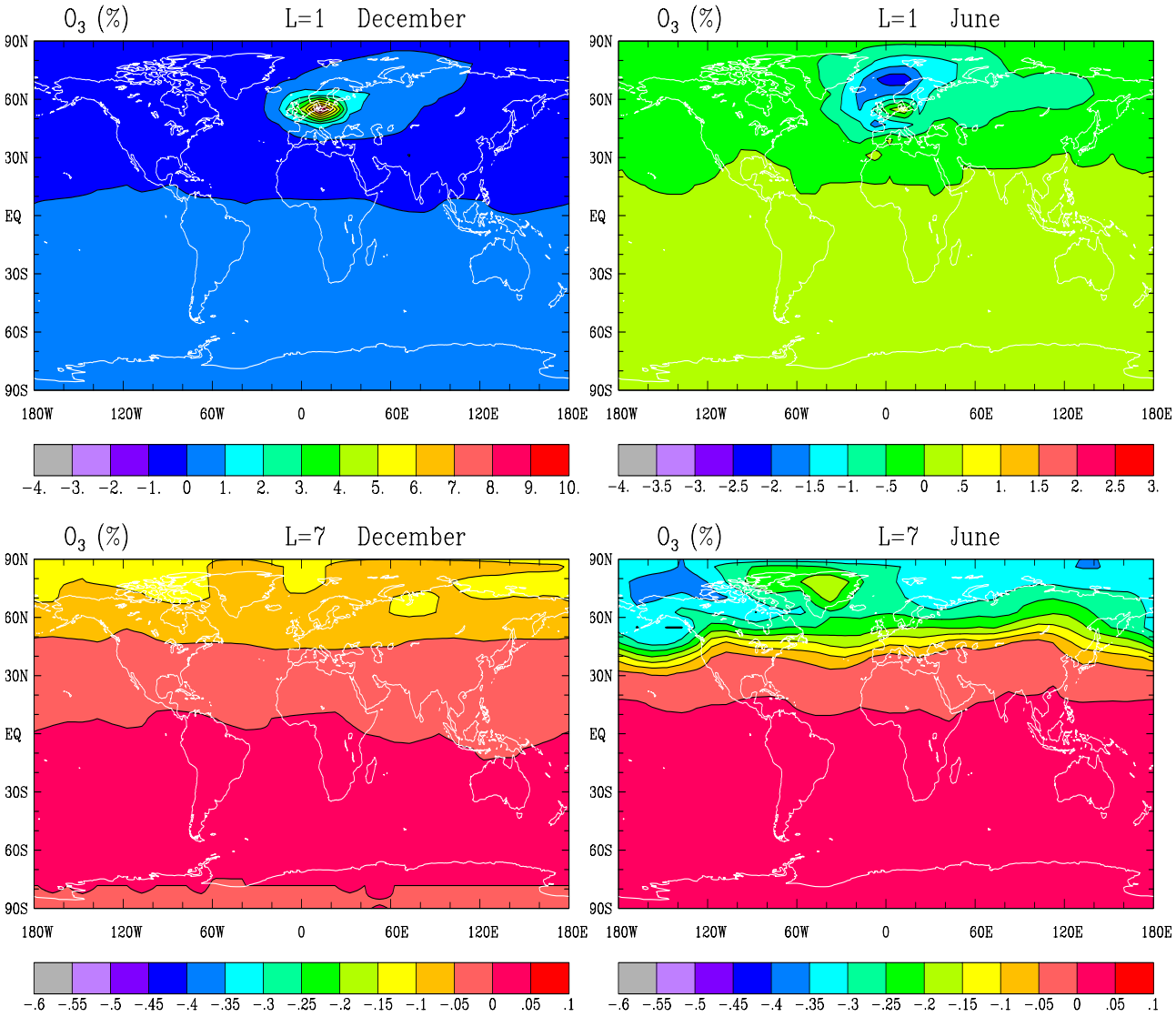

Figure 3: Calculated percentage change in the volume mixing ratio ozone for group 3 (Central Europe) at the surface (L=1), and in the upper free troposphere (L=7, approx. 12 km altitude) for December and June.

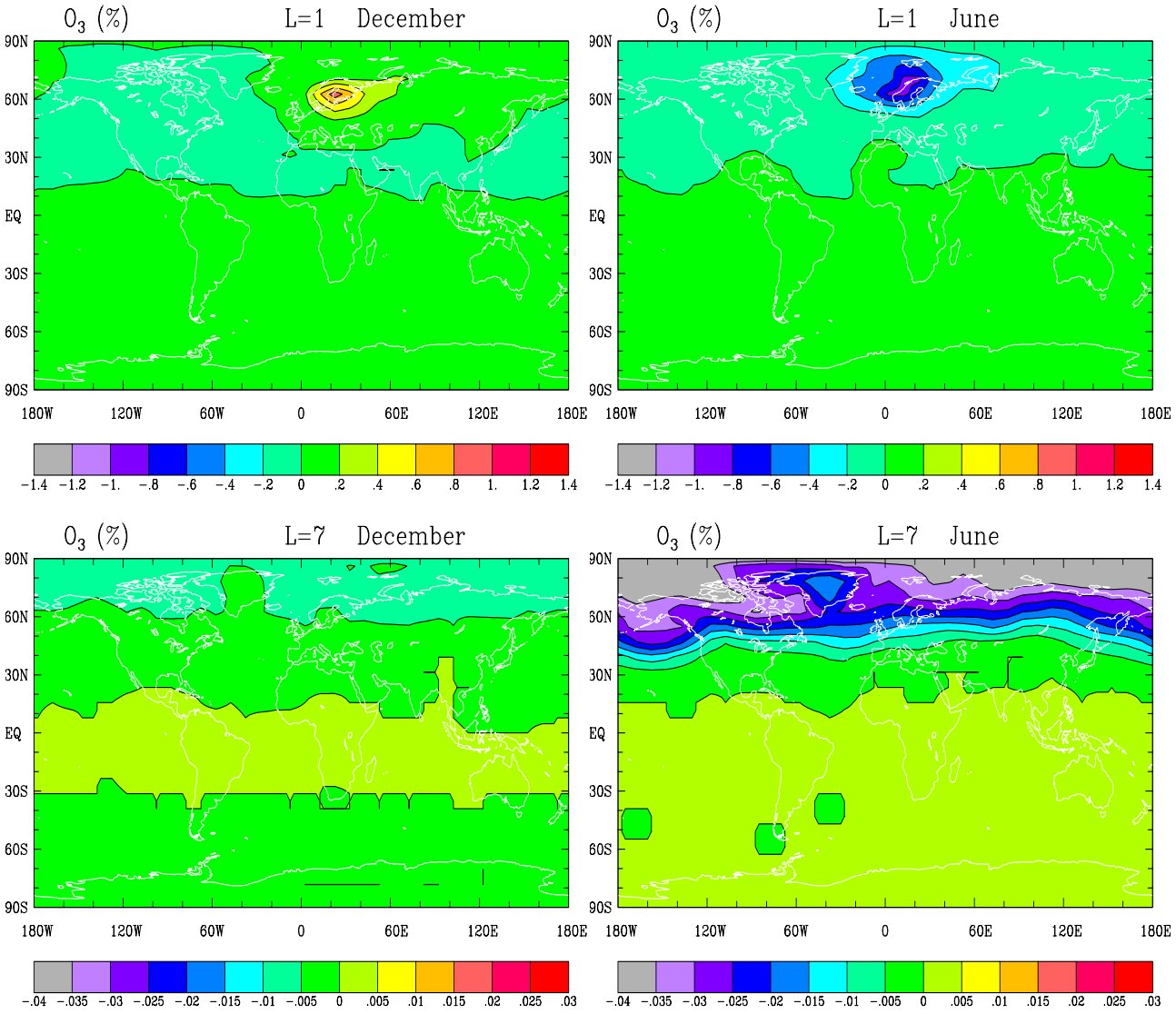

Figure 4: Calculated percentage change in the volume mixing ratio ozone for group 4 (Scandinavia) at the surface (L=1), and in the upper free troposphere (L=7, approx. 12 km altitude) for December and June.

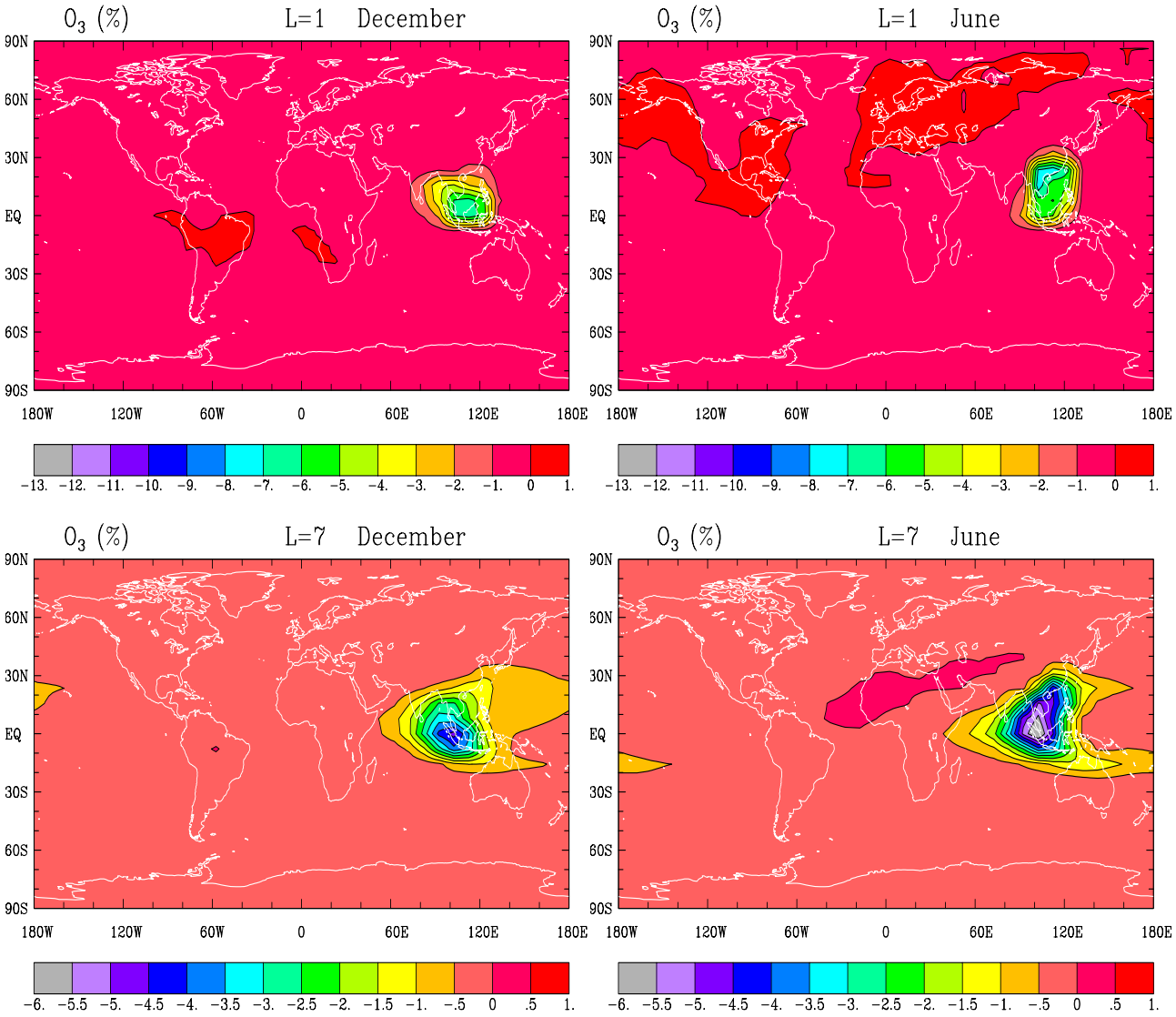

Figure 5: Calculated percentage change in the volume mixing ratio ozone for group 5 (South East Asia) at the surface (L=1), and in the upper free troposphere (L=7, approx. 12 km altitude) for December and June.

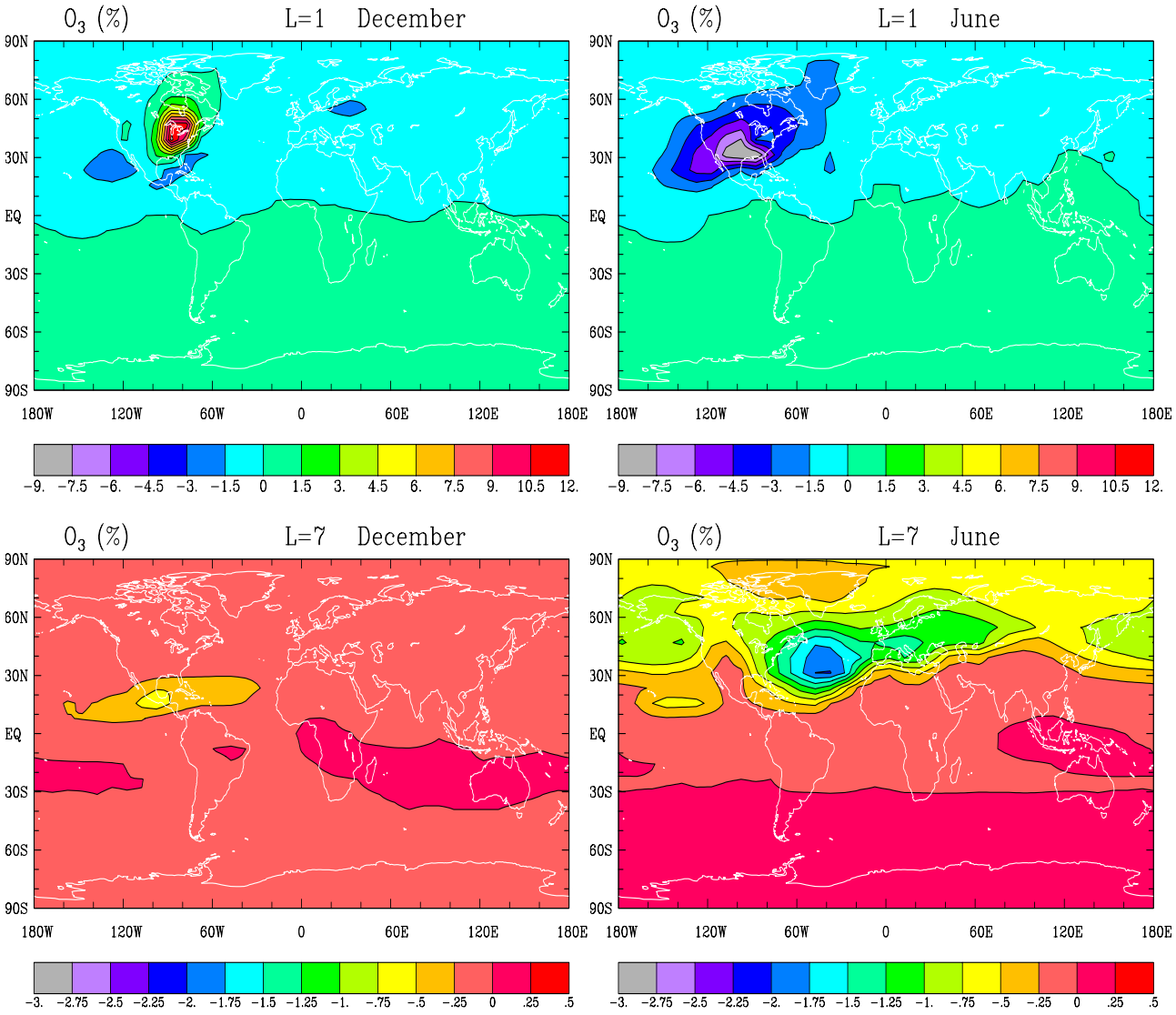

Figure 6: Calculated percentage change in the volume mixing ratio ozone for group 6 (USA) at the surface (L=1), and in the upper free troposphere (L=7, approx. 12 km altitude) for December and June.

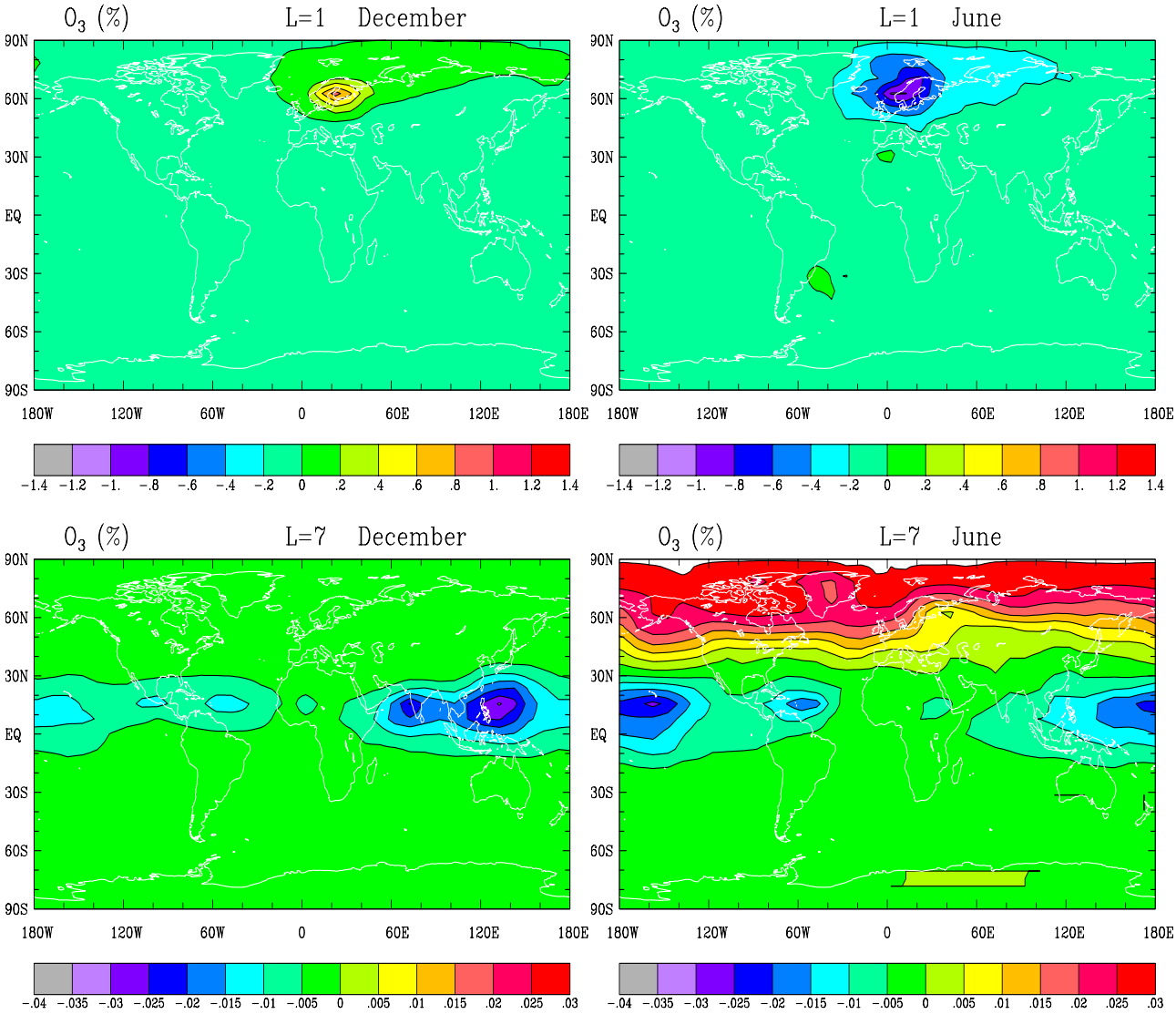

Figure 7: Calculated percentage change in the volume mixing ratio ozone for group 4 (Scandinavia), test 2 (20% reduction in NOx-emissions and 30% reductions in VOC and CO emissions) at the surface (L=1), and in the upper free troposphere (L=7, approx. 12 km altitude) for December and June.

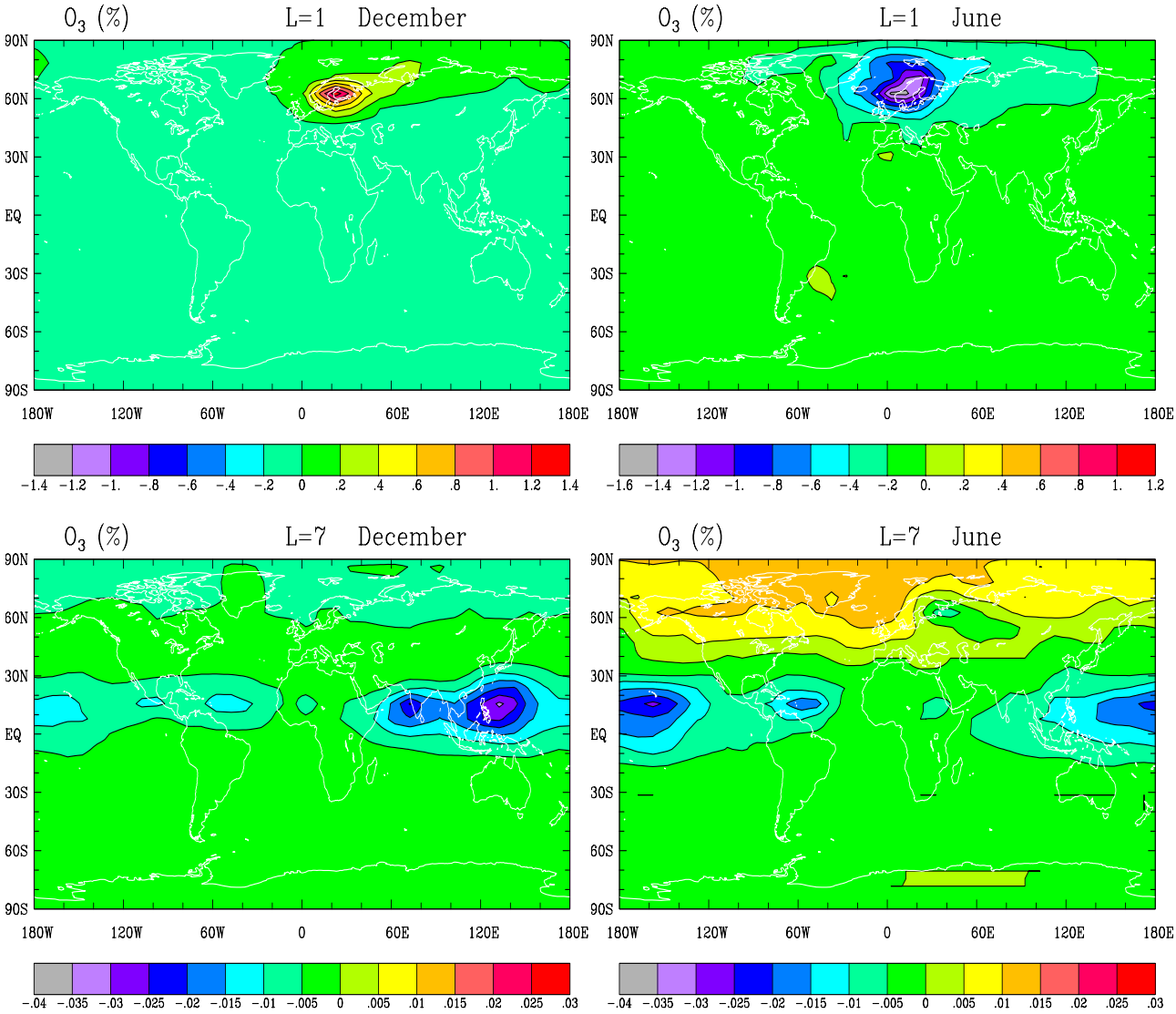

Figure 8: Calculated percentage change in the volume mixing ratio ozone for group 4 (Scandinavia), test 3 (30% reduction in NOx-emissions and 30% reductions in VOC and CO emissions) at the surface (L=1), and in the upper free troposphere (L=7, approx. 12 km altitude) for December and June.